JGR Biogeosciences

RESEARCH ARTICLE
10.1029/2022JG006889

The Impact of Freeze-Thaw History on Soil Carbon Response to Experimental Freeze-Thaw Cycles

Erin C. Rooney[1,2], Vanessa L. Bailey[2], Kaizad F. Patel[2], Angela R. Possinger[3], Adrian C. Gallo[4], Maya Bergmann[1], Michael SanClements[5], and Rebecca A. Lybrand[1,6]

[1]Department of Crop and Soil Science, Oregon State University, Corvallis, OR, USA, [2]Earth and Biological Sciences Directorate, Pacific Northwest National Laboratory, Richland, WA, USA, [3]Forest Resources and Environmental Conservation, Virginia Tech, Blacksburg, VA, USA, [4]Department of Forest Engineering, Resources, and Management, Oregon State University, Corvallis, OR, USA, [5]Battelle, National Ecological Observatory Network (NEON), Boulder, CO, USA, [6]Department of Land, Air, and Water Resources, University of California-Davis, Davis, CA, USA

Key Points:

- A combination of freeze-thaw history and soil properties dictated soil response to experimental freeze-thaw cycles
- The two soils with the least prior freeze-thaw showed diverging responses to freeze-thaw, likely due to soil moisture and mineralogy
- Future increases in freeze-thaw in both the active layer and thawing permafrost may result in contrasting carbon responses across sites

Supporting Information:

Supporting Information may be found in the online version of this article.

Correspondence to:

E. C. Rooney,
Erin.Rooney@oregonstate.edu

Citation:

Rooney, E. C., Bailey, V. L., Patel, K. F., Possinger, A. R., Gallo, A. C., Bergmann, M., et al. (2022). The impact of freeze-thaw history on soil carbon response to experimental freeze-thaw cycles. *Journal of Geophysical Research: Biogeosciences*, *127*, e2022JG006889. https://doi.org/10.1029/2022JG006889

Received 7 MAR 2022
Accepted 2 MAY 2022

Author Contributions:

Conceptualization: Erin C. Rooney, Adrian C. Gallo, Rebecca A. Lybrand
Formal analysis: Erin C. Rooney, Kaizad F. Patel, Angela R. Possinger, Maya Bergmann
Funding acquisition: Erin C. Rooney, Vanessa L. Bailey, Michael SanClements, Rebecca A. Lybrand
Investigation: Erin C. Rooney
Methodology: Erin C. Rooney, Adrian C. Gallo, Maya Bergmann, Michael SanClements, Rebecca A. Lybrand

Abstract Freeze-thaw is a disturbance process in cold regions where permafrost soils are becoming vulnerable to temperature fluctuations above 0°C. Freeze-thaw alters soil physical and biogeochemical properties with implications for carbon persistence and emissions in Arctic landscapes. We examined whether different freeze-thaw histories in two soil systems led to contrasting biogeochemical responses under a laboratory-controlled freeze-thaw incubation. We investigated controls on carbon composition through Fourier-transform ion cyclotron resonance mass spectrometry (FT-ICR-MS) to identify nominal carbon oxidation states and relative abundances of aliphatic-type carbon molecules in both surface and subsurface soils. Soil cores (~60 cm-depth) were sampled from two sites in Alaskan permafrost landscapes with different *in situ* freeze-thaw characteristics: Healy (>40 freeze-thaw cycles annually) and Toolik (<15 freeze-thaw cycles annually). FT-ICR-MS was coupled with *in situ* temperature data and soil properties (i.e., soil texture, mineralogy) to assess (a) differences in soil organic matter composition associated with previous freeze-thaw history and (b) sensitivity to experimental freeze-thaw in the extracted cores. Control (freeze-only) samples showed greater carbon oxidation in Healy soils compared with Toolik, even in lower mineral horizons where freeze-thaw history was comparable across both sites. Healy showed the most loss of carbon compounds following experimental freeze-thaw in the lower mineral depths, including a decrease in aliphatics. Toolik soils responded more slowly to freeze-thaw as shown by intermediary carbon oxidation distributed across multiple carbon compound classes. Variations in the response of permafrost carbon chemistry to freeze-thaw is an important factor for predicting changes in soil function as permafrost thaws in high northern latitudes.

Plain Language Summary As global warming progresses, permafrost (soils frozen for two or more consecutive years) is undergoing thaw. However, the process of permafrost thaw is more than a simple transition from frozen to thawed. Instead, thawing permafrost undergoes repeated freeze-thaw cycles on an annual, seasonal, and daily basis. Freeze-thaw cycles impact soils by changing soil nutrient availability and biological activity with implications for carbon decomposition. We investigated two types of freeze-thaw response: (a) how previous freeze-thaw history influenced current soil function and (b) how soils responded to experimental freeze-thaw. We tested both types of soil response to freeze-thaw cycles by evaluating the chemical composition of soil carbon. We found that soil response to freeze-thaw differed by site, even in the lower soil depths with little exposure to prior freeze-thaw. Our findings indicate that as permafrost thaws and begins to undergo freeze-thaw cycles, the response to those freeze-thaw cycles may differ by site. Variation in soil response could play a crucial role in predicting greenhouse gas emissions and rates of emission from thawing Arctic landscapes.

1. Introduction

Freeze-thaw cycles are a deformation process that shape soil function in warming permafrost landscapes and represent an intrinsic component of thaw (Henry, 2008; Ping et al., 2015; Yi et al., 2015). Freeze-thaw occurs in the surface or subsurface of the active layer during any season depending on air temperature, snowpack, and organic mat thickness (Boswell, Thompson, et al., 2020; Ping et al., 2015; Sharratt et al., 1992). Disturbance from freeze-thaw alters the soil environment through the reorganization of the physical soil structure (Konrad & McCammon, 1990; Ma et al., 2021; Rooney et al., 2022), increases in extractable carbon and nitrogen as well as

Project Administration: Vanessa L. Bailey
Resources: Vanessa L. Bailey, Michael SanClements, Rebecca A. Lybrand
Supervision: Vanessa L. Bailey, Kaizad F. Patel, Rebecca A. Lybrand
Visualization: Erin C. Rooney, Vanessa L. Bailey, Kaizad F. Patel, Angela R. Possinger
Writing – original draft: Erin C. Rooney
Writing – review & editing: Erin C. Rooney, Vanessa L. Bailey, Kaizad F. Patel, Angela R. Possinger, Adrian C. Gallo, Maya Bergmann, Michael SanClements, Rebecca A. Lybrand

higher solute concentrations (Bing et al., 2015; Patel et al., 2021), and microbial death and stimulated activity following cell lysis (Blackwell et al., 2010; Schimel & Clein, 1996), with potential implications for permafrost soil carbon loss. As the Arctic continues to warm, projected increases in freeze-thaw cycle frequency and permafrost thaw make soil response a critical component for predicting soil carbon-climate feedbacks. While the effect of experimental freeze-thaw has been studied in the active layer (Gao et al., 2021; Larsen et al., 2002; Schimel & Mikan, 2005) and permafrost (Rooney et al., 2022) separately, we still need to identify how freeze-thaw dynamics manifest collectively as a function of freeze-thaw history, soil type, and depth. Prior work demonstrated the importance of site and soil properties for predicting how permafrost soils will adapt to a warming climate (Chou & Wang, 2021; Guo & Wang, 2013; Park et al., 2015; Wang et al., 2019). The interaction of freeze-thaw history with soil properties requires further examination to expand our understanding of how the permafrost carbon cycle, including carbon chemistry, will respond to the occurrence of more freeze-thaw cycles predicted with climate change (Henry, 2008; Yi et al., 2015).

Freeze-thaw disturbance presents important implications for mineral-organic matter associations in both non-permafrost and permafrost soils (Bailey et al., 2019; G.-P. Wang et al., 2007; Yu et al., 2010). An experiment using wetland soils in the Sanjiang Plain of Northeast China (mean annual temperature of 3°C) found that freeze-thaw cycles increased sorption of dissolved organic carbon and suggested that changes to the physical structure of soil components (such as hydrous mica) increased the mineral surface area and sorption positions available to carbon (Yu et al., 2010). The study also found evidence that cumulative freeze-thaw effects on mineralogy could include greater concentrations of amorphous iron oxides, with additional contributions to the increased sorption capacity of soils. Carbon response to freeze-thaw also influenced soil aggregates, including the deformation and physical structure of aggregates through aggregate breakage and decreased water stability (Bailey et al., 2019). A study in Prince Edward Island found that the vulnerability of soils to aggregate breakage under freeze-thaw was lower in soils containing higher clay and oxide contents relative to coarse soil textures (Edwards, 2013). The changes to aggregate structure result in more stable aggregates remaining intact following freeze-thaw disturbance (Bailey et al., 2019). Furthermore, changes to aggregate stability and organo-mineral associations may affect carbon chemistry due to changes in the protection of organic matter through physical occlusion in aggregates or sorption of compounds (von Lützow et al., 2007). The influence of freeze-thaw on soil has been demonstrated previously in controlled laboratory experiments (i.e., Henry, 2007; Wang et al., 2014; Liu et al., 2021; Ma et al., 2021; Rooney et al., 2022) and field experiments (Arndt et al., 2020; Boswell, Balster, et al., 2020; Patel et al., 2018). Yet, identifying how previous freeze-thaw history influences carbon chemistry across thawing permafrost landscapes remains understudied.

Recent advances in analytical techniques and capabilities have provided molecular-scale insight into the soil chemical composition of permafrost landscapes with important advancements that support the study of freeze-thaw dynamics (Antony et al., 2017; Leewis et al., 2020; MacDonald et al., 2021; Textor et al., 2019). Fourier transform ion cyclotron resonance mass spectrometry (FT-ICR-MS) has been employed to: investigate and compare organic matter composition across a range of permafrost landscapes in the western Canadian Arctic (MacDonald et al., 2021), identify drivers of biodegradability in the soil organic matter of thawing Arctic permafrost (Textor et al., 2019), and detect dissolved organic matter transformations by microbial communities in Antarctic snowpack (Antony et al., 2017). The capabilities of FT-ICR-MS are centered around identifying the presence of unique molecular formulae within soil extracts (Kujawinski et al., 2002). Previous work coupled molecular formulae with calculations of the nominal oxidation state of carbon (NOSC), aromatic indices (AI_{mod}), as well as hydrogen to carbon (H:C) and oxygen to carbon (O:C) ratios to characterize the thermodynamic favorability and relative contribution of carbon compound classes across water-extractable organic carbon (LaRowe & van Cappellen, 2011; Seidel et al., 2014). Carbon compound classes and NOSC were used to compare the carbon chemistry and metabolism of permafrost ranging from 19,000 to 33,000 years in age (Leewis et al., 2020). The authors found that both permafrost age and paleoclimate influenced the molecular composition of carbon with NOSC decreasing as permafrost age increased. Thaw in older permafrost soils may trigger a faster microbial response than in younger permafrost soils due to differences in the composition and bioavailability of the carbon pool with age (Leewis et al., 2020). Comparisons of permafrost carbon chemistry in the western Canadian Arctic also revealed compositional differences associated with parent material and past soil modification processes including thaw, peat formation, and permafrost aggradation (MacDonald et al., 2021). Interestingly, the effect of freeze-thaw disturbance on the molecular characteristics of organic carbon remains unexamined in the Arctic,

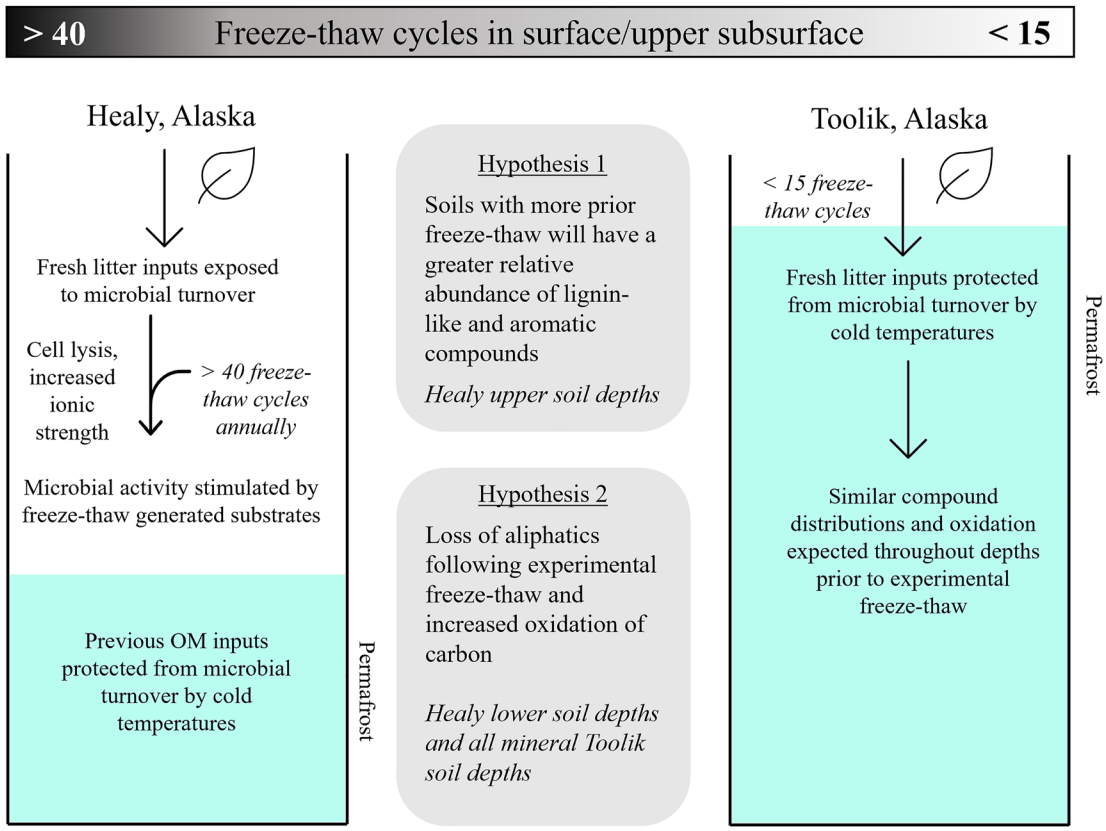

Figure 1. Visual hypothesis: Left soil profile is a high freeze-thaw frequency site (Healy), and the right profile is a low freeze-thaw frequency site (Toolik). Freeze-thaw cycles across both sites were measured via the *FTCQuant* package in R (Boswell, Thompson, et al., 2020) using temperature data from the National Ecological Observatory Network (National Ecological Observatory Network., 2021).

which is needed to assess soil response to increased freeze-thaw in permafrost environments under warming climate conditions.

The objective of this research was to determine how freeze-thaw history influenced the response of soil organic matter to experimental freeze-thaw disturbance as examined through a laboratory incubation experiment. We used upland permafrost soils from Alaska with contrasting freeze-thaw histories to test two hypotheses (Figure 1) (National Ecological Observatory Network., 2021). H1: Soil depths at Healy and Toolik with the highest previous freeze-thaw frequency (Healy mineral depths and Toolik organic depth) will be composed of more lignin-like and aromatic compounds due to preferential turnover of simple aliphatic compounds during prior freeze-thaw or extended periods of thaw. H2: Following experimental freeze-thaw, soil with little freeze-thaw history (all mineral depths at Toolik and the lower mineral depth at Healy) will show a decrease in the aliphatic pool compared with the lignin-like and aromatic carbon pools, as microbial death and lysis would provide substrates that stimulate activity of the remaining microbes. We also expected that freeze-thaw would result in an overall increase in the oxidation of carbon molecules, likely as a result of carbon desorption associated with ionic fluctuations. We used FT-ICR-MS to characterize the soil carbon composition (i.e., aliphatic and lignin-like compounds) and combined this information with soil physical and mineralogical properties (i.e., texture, mineralogical abundance, and iron/aluminum crystallinity) to test the effects of freeze-thaw history, soil type, depth and experimental freeze-thaw on carbon chemistry in permafrost-affected soils. Here, we specifically define permafrost carbon chemistry as the identified molecules in water-extractable soil organic carbon resolved by FT-ICR-MS. Our findings contribute to an improved understanding of how thawing permafrost soils will respond to the increase in freeze-thaw cycles expected during warming as well as how that response may vary based on the history of a site including previous exposure to freeze-thaw.

2. Materials and Methods

2.1. Site Description and Soil Sampling

We selected two sites along a latitudinal temperature gradient in Alaska: Toolik and Healy, both of which are part of the National Ecological Observatory Network (NEON) and have permafrost within two meters of the surface. Both sites are in tussock tundra with slopes of <3%. The sites exhibit differences in mean annual temperature (MAT) with slight variations in mean annual precipitation (MAP) (Figure S1; Table S1 in Supporting Information S1). Toolik has a MAT of −9°C and a MAP of 31.6 cm compared to Healy with mean values of −1.3°C and a MAP of 38.5 cm, respectively.

The Toolik core collection site (lat 68.66045, lon −149.37013) is located in tussock tundra in the Arctic foothills of the Brooks Range. Toolik falls within the Philip Smith Mts. quadrangle (Quaternary) composed of unconsolidated surficial alluvial and glacial deposits (Brosgé et al., 2001; Wilson et al., 2015). Vegetation includes dwarf shrubs, sedge, and herbaceous plants. Species include *Eriophorum vaginatum* (tussock cottongrass), *Carex* sp. (true sedges), and *Vaccinium vitis-idaea* (lingonberry) (National Ecological Observatory Network, 2019). The soils at the sampling location were mapped as Typic Histoturbels, which are soils with thick organic horizons that present evidence for cryoturbation and permafrost in the subsurface (National Ecological Observatory Network, 2019).

The Healy core collection area (lat 63.87980, lon −149.21539) occurs in a tussock tundra in central Alaska that is dominated by dwarf shrubs and sedge meadows (National Ecological Observatory Network, 2019). Species include *Betula glandulosa* (American dwarf birch), *Picea glauc*a (white spruce), and *Ledum palustre* (marsh Labrador tea) (National Ecological Observatory Network, 2019). The site falls within the Healy quadrangle and has been characterized as Nenana Gravel (Tertiary, Pliocene, and upper Miocene) with a composition of poorly to moderately consolidated conglomerate and coarse-grained sandstone with interbedded mudflow deposits and thin claystone layers, and local thin lignite beds (Csejtey et al., 1992; Wilson et al., 2015). Similar to Toolik, the soils at the sampling location were also classified as Typic Histoturbels (National Ecological Observatory Network, 2019).

Three permafrost cores (one meter depth) were sampled from each field site (Toolik and Healy) for a total of six cores. The cores were collected within the footprint of the NEON flux towers in April of 2016. Cores were extracted using a Gidding's probe (Giddings Machine Company, Windsor, CO, USA). At Toolik, cores were extracted from tundra on the shoulder near the base of a plateau on an east facing slope. At Healy, cores were extracted from a flat tundra with sparse small spruce. Cores were shipped frozen to Oregon State University (OSU) and preserved at −40°C.

2.1.1. Calculating *In Situ* Freeze-Thaw Cycles

The freeze-thaw cycle calculation method was adapted and modified from Rooney et al. (2022) using the FTCQuant R package (Boswell, Thompson, et al., 2020). The number of freeze-thaw cycles was calculated by season (fall, Sept-Nov; winter, Dec-Feb; spring, Mar-May; summer, June-Aug) from three years of collected data (temperature data available from NEON years 2018, 2019, and 2020). The *FTCQuant* package requires the selection of freeze-thaw cycle magnitude and duration to define a freeze-thaw cycle. We defined freeze-thaw cycles as soil temperature fluctuations persisting for a minimum of four hours < −1.5°C and a minimum of four hours >0°C (Elliott & Henry, 2009; Henry, 2007; Rooney et al., 2022). We used soil temperature data for each site (National Ecological Observatory Network., 2021) to calculate *in situ* freeze-thaw cycle counts. Sensors (Thermometrics - Climate RTD 100-ohm Probes) were placed at 5-cm increments in the top 10 cm, and then at 10-cm increments in the 10–80 cm depths. Data were collected by NEON in 30-minute increments for each depth from continuous temperature measurements averaged and recorded every 30 min. Individual sensor data were excluded if 3% or more of measurement time points were missing within each analysis time frame. The method ensured that there would be a minimum of one to five usable time series measurements for each depth by season combination. Freeze-thaw counts from 2018 to 2020 were used to infer general characterizations of different freeze-thaw histories across sites and depths.

Table 1
Healy and Toolik Soil Morphology With Depth (cm), Horizon Designation, and Material Type (Organic, Upper Mineral, and Lower Mineral)

Depth (cm)	Horizon designation	Material	Depth (cm)	Horizon designation	Material
Toolik Core 1			Healy Core 1		
0–10	Oa/Oi	Organic	0–12	Oe	Organic
10–30	Oe/Oa	Organic	12–24	Oa/Oejj	Organic
30–40	Oea/Bw	Organic	24–33	B/Oajj	Upper Mineral
40–60	Bw	Upper Mineral	33–50	B/Oajj	Upper Mineral
60–67	C	Lower Mineral	50–60	B/Oafjj	Lower Mineral
Toolik Core 2			Healy Core 2		
0-16	Oa/Oe/Oi	Organic	0–12	Oi/Oe	Organic
10-28	Oa	Organic	12–20	Oae	Organic
28-38	Bw	Upper Mineral	20–28	Oe/Bjj	Organic
38-44	Bjj	Upper Mineral	28–34	B/Oajj	Upper Mineral
44-58	BC/Oajj	Lower Mineral	34–47	B/Oafjj	Upper Mineral
			47–68	Bf	Lower Mineral
Toolik Core 3			Healy Core 3		
0-14	Oi	Organic	0–9	Oi	Organic
14-35	Oea	Organic	9–16	Oe	Organic
35-41	BC/Oajj	Upper Mineral	16–30	Oa/Afjj	Organic
41-50	Bw	Upper Mineral	30–38	Af	Upper Mineral
50-58	BC/Oajj	Lower Mineral	40–54	BCg	Lower Mineral

2.2. Freeze-Thaw Incubation

We conducted laboratory incubations that exposed a subset of soils from Toolik and Healy to six additional experimental freeze-thaw cycles, followed by soil chemical analyses. Parent cores ($N = 3$ for each site) were separated by morphologic horizon designation into incubation units (Table 1). All subsequent incubation experiments and soil analyses were performed on incubation units, which represented a distinct combination of depth increment and genetic horizon type (Table 1). For data interpretation and statistical analyses, incubation units were classified as follows for comparisons: All major O horizons (or combination horizons dominated by O material) were classified as "organic." All A/Bw horizons underlying the organic deposits were classified as "upper mineral" material. All Bw/C/Bf horizons beneath the upper mineral depths were classified as "lower mineral" depths.

Incubation units were incubated in 480 mL glass jars for two months. The freeze-thaw incubation parameters included a total of six freeze-thaw cycles consisting of five days for thaw (+2°C) followed by five days for freeze (−5°C), for a total of ten days per freeze-thaw cycle. Control soils kept at −5°C for a freeze-only treatment throughout the incubation. Parent core subsampling for incubation units and soil morphologic descriptions were conducted in a cold room (−10°C). Major horizons and sub horizon designations, cryostructures, and coarse fragment estimates were recorded according to Soil Survey Staff (2015), Soil Science Division Staff (2017), and Ping et al. (2015). The incubations were performed in a temperature controlled environmental chamber (Hoffman Manufacturing Inc., SG2-22 Dual Environment Controlled Chamber). Soils were preserved to the greatest degree possible during subsampling (parent core into incubation unit) to retain original soil structure (Figure S2 in Supporting Information S1). Samples were incubated at *in situ* (field moist) moisture to simulate field conditions. Due to the ample headspace of the jars, limited thaw time, and low thaw temperature (2°C), the jars were able to remain sealed for the duration of the incubation to reduce the chance for unintentional moisture loss via evaporation and to limit exposure to temperatures over 2°C. Following the incubation, soils were destructively sampled, and subsamples of each incubation unit were allocated directly to water extraction for FT-ICR-MS, or air-dried and sieved for subsequent analyses (i.e., XRD, texture, and pH/EC).

2.3. Fourier Transform Ion Cyclotron Resonance Mass Spectrometry

Following the incubation experiment, incubation units were subsampled for water extraction directly from the incubation. FT-ICR-MS analysis was performed on water-extractable organic carbon (WEOC) via automated direct infusion at the Environmental Molecular Sciences Laboratory (EMSL) in Richland, WA on a 21 T FT-ICR mass spectrometer using negative mode electrospray ionization. Soil (300 mg wet weight) was subsampled from each incubation unit and weighed into 2 mL glass vials (MicroSolv) with 1 mL of MilliQ water added. Vials were shaken on a thermal mixer (Eppendorf ThermoMixer C) for 2 hr at 448 Relative Centrifugal Force (RCF) at room temperature and then filtered through 0.45 μm Hydrophilic PTFE filters (Thermo Scientific) for WEOC extracts. The filtered extracts were prepared for FT-ICR-MS analysis using Bond Elut PPL solid phase extraction cartridges (Agilent, USA) following Dittmar et al. (2008).

WEOC extracts were diluted 1:2 (sample: methanol by volume) to aid ionization and then randomized for analysis. One hundred and forty-four individual scans were averaged for each sample to improve the overall abundance of ions detected. Peak selection and calibration filtered data to signal-to-noise ratio of 7. Datasets were aligned and formulae were assigned using the in-house *Formularity* software (Kujawinski & Behn, 2006; Tolić et al., 2017). Further data processing was performed using the *fticrrr* R package (Patel, 2020). All peaks were analyzed on a presence/absence basis with only peaks occurring in ⅔ of replicates considered to be present (Kujawinski et al., 2002). Only carbon-containing formulas between 200 and 900 m/z were included. The modified aromaticity Index (AI_{mod}) (Equation 1) was calculated for each formula to help with compound classification (Koch & Dittmar, 2006).

Aromaticity Index (AI_{mod})

$$AImod = \frac{1 + C - (0.5 \times O) - S - (0.5 \times (N + P + H))}{(C - (0.5 \times O) - S - N - P)} \quad (1)$$

Nominal Oxidation State of Carbon (NOSC)

$$NOSC = \frac{4 - (((4 \times C) + H - (3 \times N) - (2 \times O) - (2 \times S))}{C} \quad (2)$$

In which C = carbon, H = hydrogen, O = oxygen, S = sulfur, N = nitrogen, P = phosphorus.

The identified molecules were separated into four compound classes using the AI_{mod} and H/C and O/C ratios, following Seidel et al. (2014): (a) condensed aromatics ($AI_{mod} > 0.66$); (b) aromatic compounds ($0.66 > AI_{mod} > 0.50$); (c) highly unsaturated and lignin-like compounds ($AI_{mod} < 0.50$ and $H/C < 1.5$); and (d) aliphatic compounds ($>H/C \geq 1.5$) (Figure S3 in Supporting Information S1). Relative abundances were calculated as the number of unique peaks (formulas) within a specific compound class compared with the total number of unique peaks across all compound classes. We used the nominal oxidation state of carbon (NOSC, Equation 2) to analyze thermodynamic favorability of compounds to determine which compound classes and depths were most susceptible to microbial oxidation at each site. The association between NOSC and thermodynamics is based on the assumption of oxic conditions and use of oxygen as the dominant terminal electron acceptor, allowing for a relationship between Gibbs Free Energy and NOSC established in previous literature (Graham et al., 2017; LaRowe & van Cappellen, 2011).

2.4. Soil Properties and Characterization

Following the incubation, freeze-only (control) samples were subsampled for soil physical-chemical properties and analyzed for soil particle size, pH, electrical conductivity, and gravimetric moisture by the Oregon State University Soil Health Laboratory. Soil pH and electrical conductivity (EC) were measured on sieved (<2 mm), air-dried soils. Deionized water was added to the soil (1:1 w/w) to form a soil slurry and then analyzed via pH/EC meter (Hanna H15522) (Miller et al., 2013; Thomas, 2018) (Table 2). Gravimetric moisture was determined on 1–1.5 g field moist samples by oven drying for 24 hr at 105°C. Gravimetric moisture, pH, and EC were analyzed on the control samples of all depths and then pooled within each material class for statistical analysis (i.e., organic, upper mineral, lower mineral) (Table 2).

Table 2
Soil Characterization Properties for Healy and Toolik Soil Depths, Reported as Mean ± Standard Error

						Particle size analysis			
	pH	EC (dS/cm)	Soil Moisture (%)	Total C (%)	Total N (%)	Sand (%)	Silt (%)	Clay (%)	Texture Class
Healy									
Organic	4.55 ± 0.08	0.06 ± 0.01	439.19 ± 141.6	38.54 ± 1.4	1.27 ± 0.06	NA	NA	NA	NA
Upper Mineral	5 ± 0.15	0.03 ± 0	203.47 ± 9.91	20.27 ± 1.79	0.85 ± 0.09	24 ± 3	45 ± 4	31 ± 3	Clay Loam
Lower Mineral	5.36 ± 0.13	0.02 ± 0	122.8 ± 33.04	10.96 ± 0.41	0.42 ± 0.01	36 ± 5	40 ± 4	23 ± 2	Loam
Toolik									
Organic	5.07 ± 0.18	0.03 ± 0	420.73 ± 55.62	41.04 ± 0.89	1.96 ± 0.14	NA	NA	NA	NA
Upper Mineral	5.31 ± 0.09	0.02 ± 0	35.73 ± 6.91	11.34 ± 0.6	0.42 ± 0.02	47 ± 6	29 ± 1	25 ± 3	Loam
Lower Mineral	5.29 ± 0.11	0.03 ± 0	30.85 ± 4.58	11.75 ± 0.97	0.44 ± 0.05	48 ± 7	27 ± 0	25 ± 1	Sandy Clay Loam

Note. Moisture is reported as gravimetric moisture content. Particle size classes were determined only for upper and lower mineral soil depths, via the sieve and pipette method. Sand defined as 50 microns to 2 mm, silt defined as 2 to 50 microns, clay defined as <2 microns.

Particle size distribution was determined on mineral horizon samples via the sieve and pipette method for the mineral soils (Gee & Bauder, 1986; Köhn, 1928; Sheldrick & Wang, 1993). Control samples from every mineral depth were air dried and sieved to <2 mm, with two depths excluded due to too little sample mass. Both upper mineral and lower mineral depth classes had an $N = 3$ at each site, with the exception of Toolik lower mineral which had an $N = 2$ (particle size analysis only) due to a limited sample. Preceding analysis, organic matter and other cementing agents were removed from soil. Sodium hexametaphosphate was added to the soil suspension and shaken overnight. Sand size fractions were separated by wet sieving through 2000 µm, oven dried, and then sieved through a series of sieves (50–100 µm, 100–250 µm, 250–500 µm, 500–1,000 µm, and 1,000–2,000 µm). The remaining silt and clay suspension was brought to a volume of 1 liter and specific aliquots of fluid were removed by pipette at time and depth points to capture silt and clay particles in accordance with Stokes' Law (Table 2). Following data collection, particle size fractions were averaged within each depth class (i.e., upper mineral, lower mineral) (Table 1).

Following incubation, control samples only were air-dried, sieved, and ground prior to analysis for nitrogen and carbon on a Vario EL Cube Elemental Analyzer (Elementar Analysensysteme GmbH, Langenselbold, Germany). Homogenized samples were weighed and sealed into tin boats, and then combusted at 1,150°C in the presence of oxygen. The signals for nitrogen and carbon were measured using a Thermal Conductivity Detector (TCD). The detector response was calibrated using aspartic acid and validated using a soil reference material.

2.5. X-Ray Diffraction

Powder x-ray diffraction (XRD) patterns were collected from powders packed into zero-background well holders using a SmartLab SE diffractometer (Rigaku, Japan). The instrument employed Bragg-Brentano geometry with a Cu X-ray source ($\lambda = 1.5418$ Å), a variable divergence slit, and a high-speed D/teX Ultra 250 1D detector. Patterns were collected between 2 and 100° 2θ at intervals of 0.01° 2θ, scanning at 2° 2θ/min. Quantitation of minerals was performed by the Rietveld method using TOPAS (v6, Bruker AXS). This method combines calculated XRD patterns from the substituent minerals to provide the best fit with the observed pattern. For each mineral the scale factor, cell parameters (constrained within ca. 0.5% of the expected values), and crystallite size (constrained between 50 and 500 nm) were refined. For minerals with a platy morphology, a preferred orientation correction was also refined. The scale factors from the Rietveld refinement were used to determine the relative quantities of the minerals, which are presented scaled to a total of 100%.

2.6. NEON Biogeochemical Data for Soil Characterization

We accessed NEON biogeochemical data for both sites from NEON distributed plot initial characterization, which provides site-level differences for soil properties at Healy and Toolik (National Ecological Observatory Network, 2020). Dithionite citrate-extractable (DC) (captures total non-silicate crystalline iron oxides, substituted

aluminum in iron oxides, and both organically complexed and poorly crystalline iron and aluminum) as well as ammonium oxalate-extractable (AO) (captures organically complexed and poorly crystalline iron and aluminum) values were used to determine crystalline Fe + Al (Equation 3) (Figure 3; Shang & Zelazny, 2015).

Crystalline iron (Fe) and aluminum (Al)

$$Crystalline\ Fe\ +\ Al = (DC\ Fe\ -\ AO\ Fe) + (DC\ Al - AO\ Al) \quad (3)$$

2.7. Supplemental Respiration Experiment

After the freeze-thaw incubation, soils were subsampled for respiration measurements which were used determine the relationship between the FT-ICR-MS profile and response of aerobic respiration to freeze-thaw cycles. Aerobic incubations were conducted using 20–30 g of soil subsampled from select incubation units following the freeze-thaw incubation. The samples were stored in 50-mL specimen cups placed inside air-tight quart-size Mason jars that had an internal volume of 946 mL, with 2 mL of water added to the bottom of the jar to reduce evaporation. The Mason jar lids were fitted with rubber septa to collect headspace samples. The aerobic incubation was conducted over two weeks in a dark cabinet at 20°C. Gas samples were taken from the mason jars at 1, 4, 7, and 14 days and immediately analyzed on a Picarro [A0311] gas analyzer for CO_2 concentration. After each measurement, jar lids were opened, and the airspace of each jar was cleared using a laboratory vacuum at a low suction for one minute each and then left open for 10 min to allow for air circulation. Soils were maintained at their time-zero moisture content. Results from this experiment are included in Text S2 and Figure S8 of Supporting Information S1.

2.8. Statistics

FT-ICR-MS data were analyzed using univariate linear mixed-effects models (LME), permutational multivariate analysis of variance (PERMANOVA), and principal components analysis (PCA) to test the effect of site (Healy and Toolik), depth (organic, upper mineral, and lower mineral), treatment (freeze-thaw vs. control), and their interactions on the relative abundance of compound classes and the nominal oxidation state of carbon. When testing the effect of site and treatment on the NOSC of compound classes, depth was used as a random effect. For the FT-ICR-MS data, we tested the effects of site, depth, and treatment on all soil depths as well as on mineral only soil depths due to the unique behavior of organic soil horizons (with mineral-only data noted in the text). We tested the effects of site and material as well as their interaction on X-ray diffraction mineral abundances and the ratio of crystalline to poorly crystalline Fe + Al forms using analysis of variance (ANOVA). Statistical significance was determined at $\alpha = 0.05$. Data analysis and visualization were performed using R version 4.0.1 (2020-06-06) with RStudio version 1.4.1106 (R Core Team, 2020). Diffractogram patterns were visualized using the *powdR* package version 1.3.0 (Butler et al., 2021). Data processing and analysis was conducted using *dplyr v1.0.1* (Wickham et al., 2020) and *vegan v2.5-6* (Oksanen et al., 2019) packages. Data visualization was conducted using *ggplot2 v3.3.2* (Wickham, 2016) and *PNWColors* (Lawlor, 2020). All data and scripts are available at https://github.com/Erin-Rooney/FTC-FTICR and archived and searchable at https://search.emsl.pnnl.gov (Project ID #50267).

3. Results

3.1. Characterization of Control Soils

We observed evidence for contrasting freeze-thaw histories between the two study sites and as a function of depth using temperature data collected by NEON from 2018 to 2020 (Figure 2) (National Ecological Observatory Network., 2021). Healy soils experienced the greatest freeze-thaw cycle frequency, with the majority (61%–65%) of freeze-thaw cycles occurring in organic soil depths during spring (March to May). During spring, organic soils experienced >35 cycles while upper mineral soils underwent 13 cycles in both fall and spring, with the majority (8 freeze-thaw cycles) occurring in fall (Figure 2). In contrast, Toolik experienced fewer freeze-thaw cycles, with the majority of the cycles (88%–93%) occurring in the fall (<15 freeze-thaw cycles in the surface soils). The lower mineral soils experienced very few freeze-thaw cycles at both sites, approximately 1–2 per year.

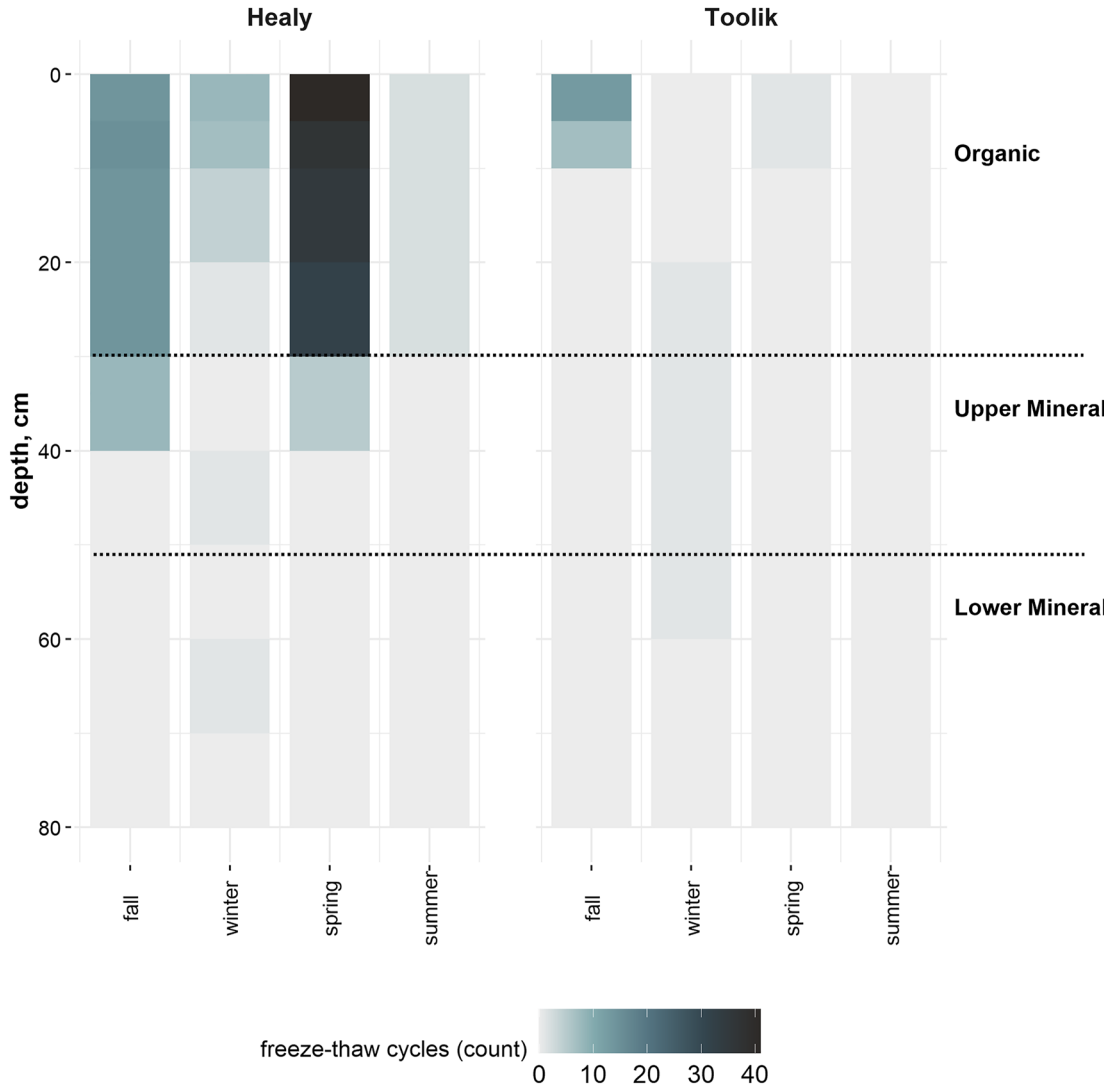

Figure 2. Short duration freeze-thaw cycles (four hours < −1.5°C and a minimum of four hours >0°C) measured by site and depth using NEON temperature data from 2018 to 2020 and calculated using the *FTCQuant* Package (Boswell, Thompson, et al., 2020).

Soil morphological observations, horizon designations, pH, EC, and texture classes were similar across sites (Tables 1–2). We observed thicker ice layers in mineral horizons at Healy (1–3 cm) compared to Toolik (<1 mm), which aligned with the large variations in gravimetric moisture percentages identified in the samples between sites (Text S1 in Supporting Information S1; Table 2). Healy and Toolik showed some contrast in soil particle size distribution across mineral soil depths, with Healy composed of clay loam and loam soils versus the loam and sandy clay loam soils identified at Toolik (Table 2). Clay percent varied from 31% to 23% in the upper and lower mineral soils at Healy, respectively, whereas clay percentages for the Toolik mineral soils remained constant at ~25% throughout.

Mineralogical composition for mineral soils at both Healy and Toolik was relatively similar with quartz and feldspar minerals comprising the most abundant mineral phases, although we did observe notable differences in mineral abundance (Figure S4 in Supporting Information S1). Toolik mineral soils were dominated by quartz (~80%), with minor amounts of mica (~6.6%), albite (~4.4%), and chlorite (~4.7%). Conversely, Healy soils contained less quartz (~46%), greater proportions of mica (~21%), and albite (~16%). When comparing mineralogical abundance between sites, Healy consistently contained more phyllosilicate (e.g., mica, kaolinite) and inosilicate minerals (e.g., hornblende) compared to Toolik (ANOVA, $P < 0.05$). Healy also contained more potassium-rich feldspar (microcline), plagioclase feldspar (albite), and chlorite compared to Toolik soils

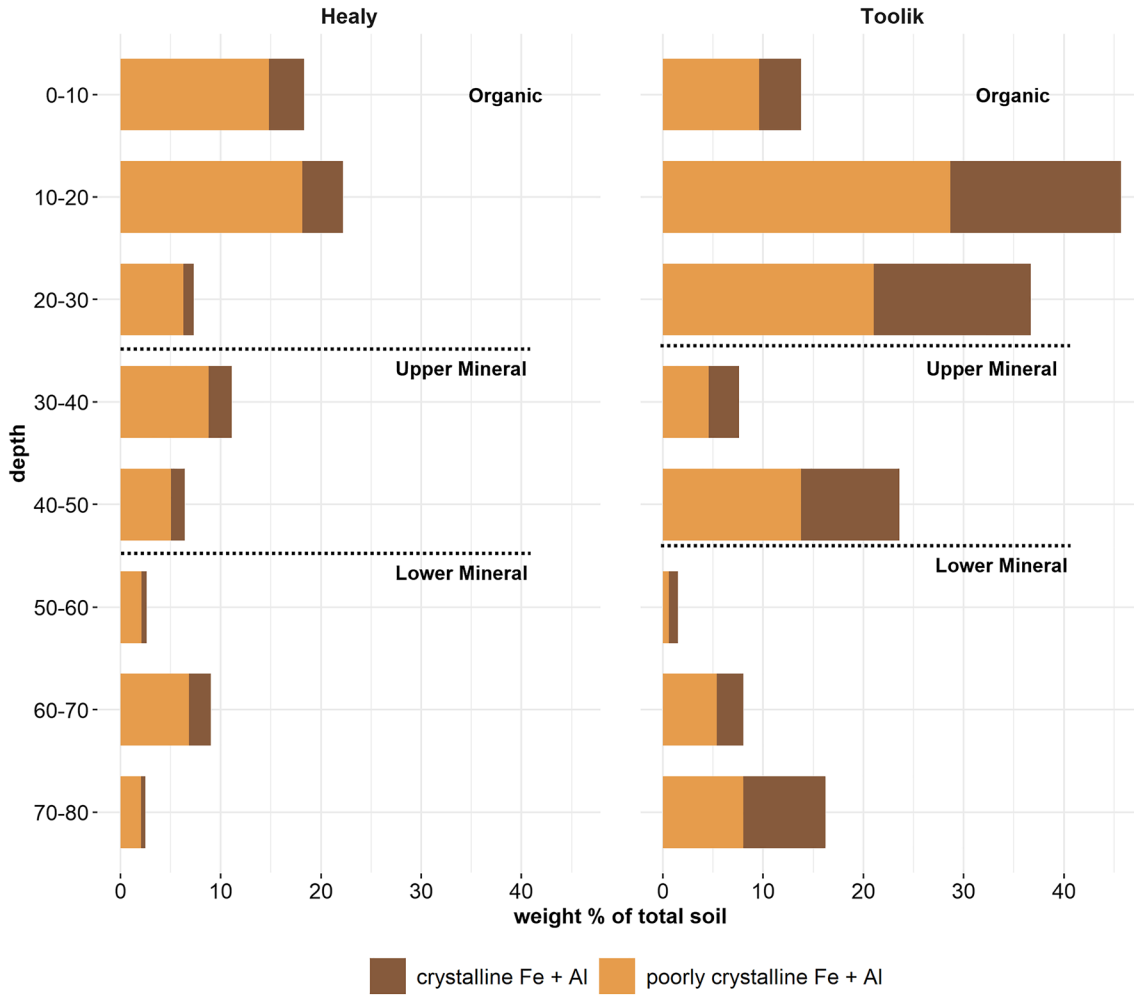

Figure 3. Crystalline and poorly crystalline iron and aluminum, reported as percent weight of soil. Toolik had a higher proportion of crystalline iron and aluminum compared with Healy, which was dominated by poorly crystalline compounds (ANOVA, $P < 0.001$). Data from NEON distributed plot soil chemistry data (National Ecological Observatory Network, 2020).

(ANOVA, $P < 0.05$) (Figure S4 in Supporting Information S1). Depth did not have a significant effect on mineral composition, nor did we find an interaction of site and depth (Figures S4–S5 in Supporting Information S1). We also integrated geochemical data generated by NEON into our analysis to compare differences in the ratio of crystalline to poorly crystalline Fe + Al forms. We found that Toolik exhibited a higher proportion of crystalline Fe + Al compounds compared with Healy, which had a higher proportion of poorly crystalline Fe + Al (ANOVA, $F = 12.726$, $P < 0.001$) (National Ecological Observatory Network, 2020) (Figure 3).

3.2. SOM Composition of Control Soils

SOM composition of the control soils (incubated as freeze-only) varied with depth (PERMANOVA, $P = 0.001$; Figure 4) but did not differ by site (PERMANOVA, $P = 0.815$). The surface organic soils showed similar chemical compositions across both sites, with lignin-like molecules comprising ~50% and aliphatic molecules comprising ~35% of the total identified peaks (Figure 5; Figure 4a). We identified a stronger separation between sites for the lower mineral soil depth versus the organic or upper mineral soils after accounting for intra-depth variability using between-site Euclidean distances (Figure 4b). The Healy lower mineral soils were strongly influenced by aromatic and lignin-like molecules compared to Toolik lower mineral soils, which were more influenced by condensed aromatic molecules (Figure 4a).

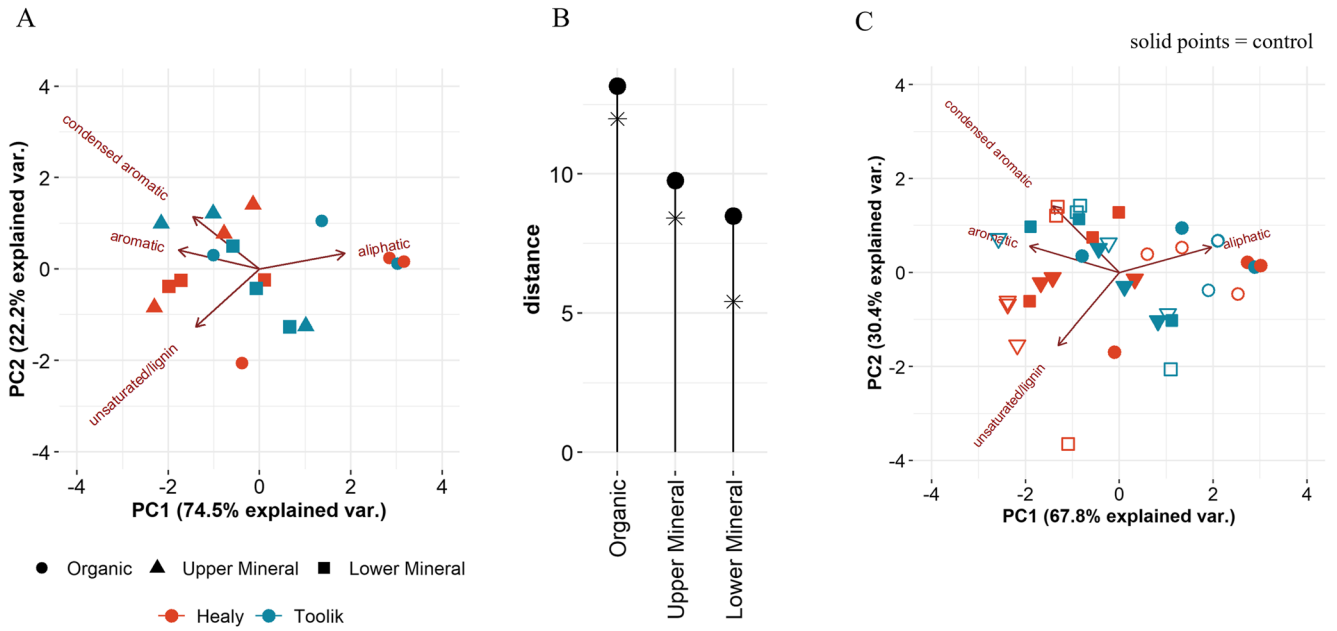

Figure 4. (a) Principal Components Analysis biplot of FT-ICR-MS data showing separation by site for control samples. (b) Euclidean distances between sites for each soil depth (controls only). Black stars indicate intra-depth variability at each site whereas the black circles represent the Euclidean distance between sites at each depth. (c) Principal Components Analysis biplot of FT-ICR-MS data showing separation by site for all samples. Solid points = control (freeze-only) samples, open points = freeze-thaw treated samples.

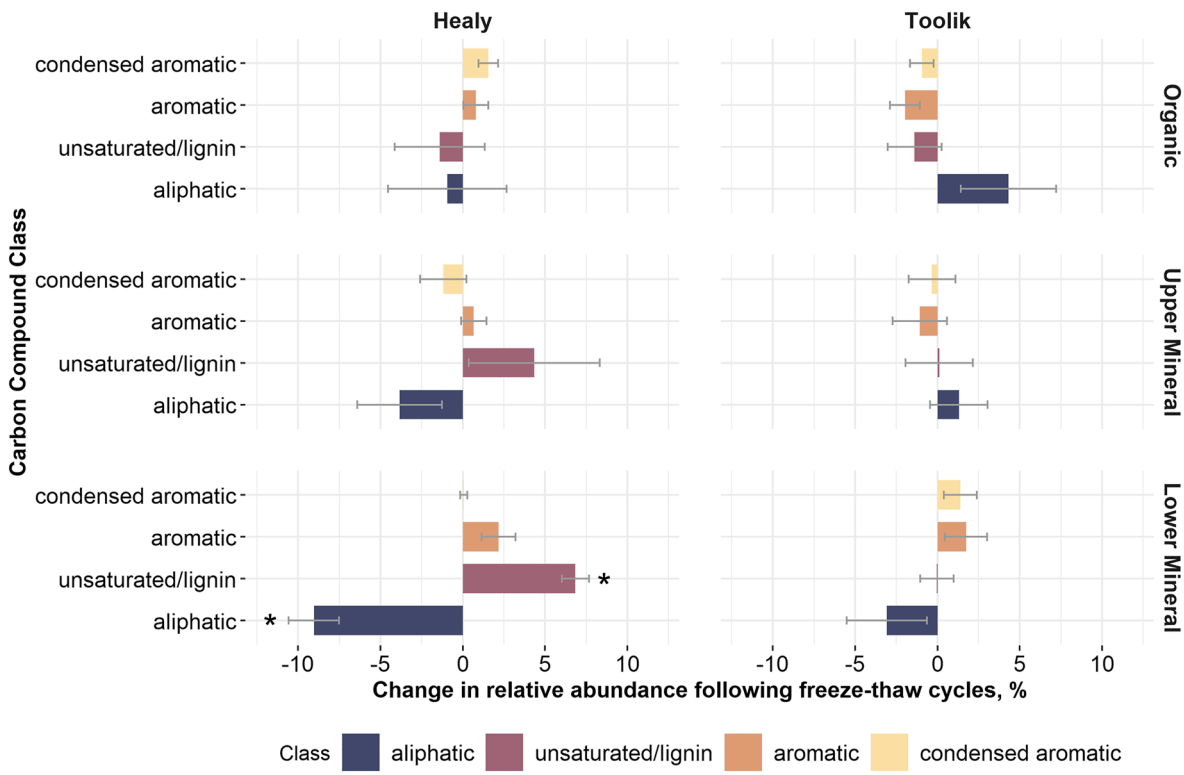

Figure 5. The change in relative abundances (percentage) of carbon compound classes following freeze-thaw cycles within each material grouping from Healy and Toolik. Asterisks denote significant differences between control and freeze-thaw, at $\alpha = 0.05$. Error bars represent standard error calculated by propagation of error.

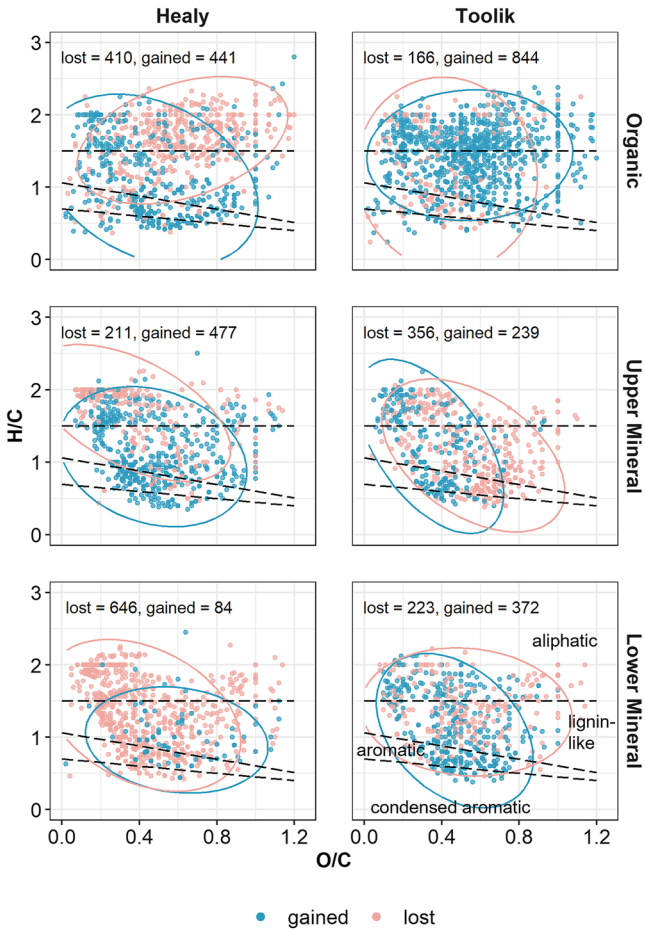

Figure 6. Van Krevelen plots showing organic compounds gained (newly identified) and lost following freeze-thaw, by site and depth. Molecules are plotted as functions of their H-to-C and O-to-C ratios. Ellipses represent 95% confidence intervals. See Figure S3 in Supporting Information S1 for illustration of van Krevelen diagram interpretation.

3.3. SOM Composition Following Experimental Freeze-Thaw

The freeze-thaw laboratory incubations caused shifts in the FT-ICR-MS-resolved SOM composition in the lower mineral horizons at Healy (Figures 4c and 5). Following the freeze-thaw incubations, the organic horizon soils at both sites remained strongly influenced by aliphatic molecules following freeze-thaw at both sites (~35–38% across both Toolik and Healy), with as much intra-site variability as inter-site variability in organic depths (Figure 4c, Figure S6 in Supporting Information S1). There was a stronger separation by site in the lower mineral depths (Figure 4c). For example, Healy soils exhibited an increase of ~7% in the relative abundance of lignin-like molecules and a decrease of ~9% in aliphatics whereas Toolik soils experienced only minor, non-significant changes in the relative abundances of the compound classes (Figures 4c and 5). The supplemental respiration experiment showed carbon losses as CO_2 from both Healy and Toolik, with the largest CO_2 production occurring during days 1 and 4 in control samples from Toolik's lower mineral depths. In contrast, Healy showed the largest concentration of CO_2 during day 1 in the lower mineral freeze-thaw samples (Figure S8 in Supporting Information S1).

We found that sample depth had a larger effect on FT-ICR-MS resolved SOM composition compared to site or freeze-thaw treatment when including organic as well as mineral horizons in the PERMANOVA analysis. Sample depth accounted for 12% of total variation in compound classes across all samples (PERMANOVA, $P = 0.01$) and site accounted for 5% of variation ($P = 0.07$) whereas freeze-thaw did not have a significant effect on SOM composition ($P = 0.545$). When we analyzed only the mineral soil depths, site accounted for 17% of total variation ($P = 0.031$), whereas freeze-thaw still did not have a significant effect (PERMANOVA, $P = 0.231$). Notably, the PCA showed a greater separation of control versus freeze-thaw soils in the lower mineral depth of Healy relative to intra-treatment variability. All other depths within both sites had as much intra-treatment variability as distance between freeze-thaw and control, with no significant effect of the interaction between freeze-thaw treatment and site ($P = 0.3$; Figure 4c, Figure S6 in Supporting Information S1).

The Healy organic and mineral soils showed strong shifts in SOM composition following freeze-thaw incubation (Figures 6 and 7). Following experimental freeze-thaw, Healy upper mineral soils experienced a net increase in the unique peaks identified, as peaks were lost from the aliphatic and lignin-like regions, and new peaks were identified in the same regions. In contrast, the Healy lower mineral soils experienced a net loss in peaks identified, as peaks were mostly lost from all regions. Additionally, the loss and gain of unique compounds across Healy's organic, upper mineral, and lower mineral depths follow a sequential shift. The gained peaks in the organic and upper mineral depths overlap with the lost peaks in the upper mineral and lower mineral depths, respectively (Figure 6). It is important to note that organic carbon was not standardized during FT-ICR-MS analysis. It is likely that some peak count differences may be attributed to variability in SOM content across samples, although the low variability within depth classes and across the organic and lower mineral depths of both sites (Table 2) reduces this concern. In addition to changes in peak count following freeze-thaw, there were shifts in the NOSC values of the identified peaks. Prior to freeze-thaw, Healy had higher NOSC values at all three depths compared with Toolik (LME, $P < 0.005$) (Figure S7 in Supporting Information S1). Following freeze-thaw, Healy upper mineral soils experienced a net gain of identified molecules (477 peaks), whereas the lower mineral soils experienced a net loss (646 peaks) (Figure 6), with site, treatment, and depth having variable effects on NOSC values of gained and lost compounds. In Toolik, increased NOSC occurred in aliphatic compounds gained following freeze-thaw. Conversely, increases in NOSC for the Healy samples only occurred in the aromatic and lignin-like compounds gained following freeze-thaw (Figure 8).

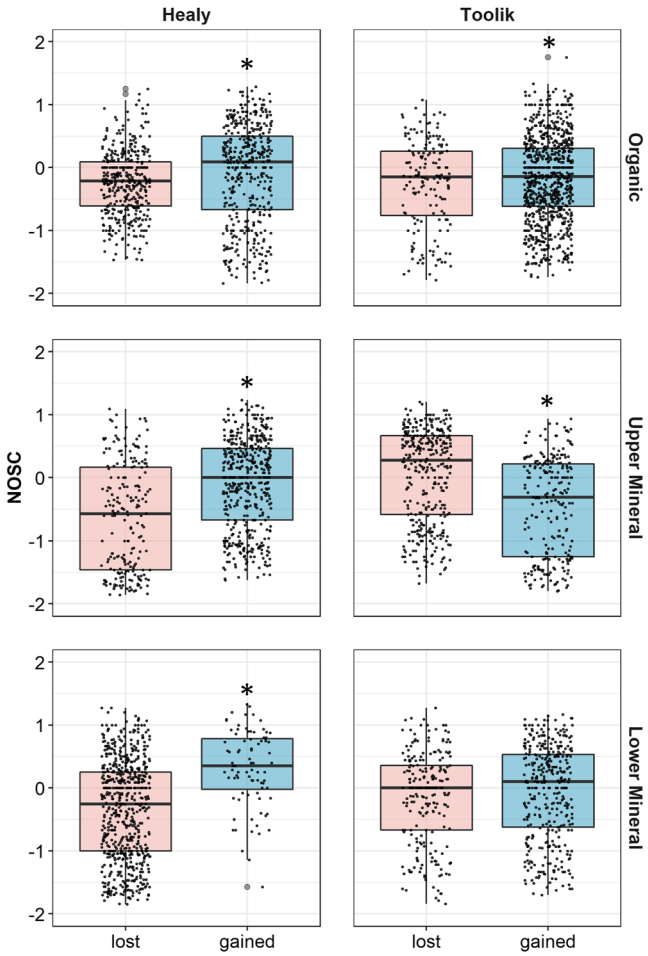

Figure 7. Nominal oxidation state of carbon (NOSC) for molecules lost or gained (newly identified) following freeze-thaw, by site and depth. Asterisks denote statistically significant differences between treatments at $\alpha = 0.05$. For Healy soils, NOSC of newly identified compounds was greater than NOSC of compounds lost, for all depths. For Toolik organic soils, NOSC of gained > lost, whereas for Toolik upper mineral soils, NOSC of lost > gained following freeze-thaw.

4. Discussion

4.1. Freeze-Thaw History and SOM Composition

The recent freeze-thaw history captured by available NEON soil temperature data (2018-2020) and our *FTCQuant* analysis (Boswell, Thompson, et al., 2020) indicated the largest difference in prior freeze-thaw occurred between organic horizons at Healy and Toolik. We detected evidence for ~40 annual freeze-thaw cycles in organic soils from Healy versus ~15 annual freeze-thaw cycles in those from Toolik. However, the organic soils from both sites were the most compositionally similar, with comparable relative abundances of lignin-like compounds and aliphatics. We made similar observations for the upper mineral soils, which again differed by site in terms of prior freeze-thaw but were compositionally similar.

Hypothesis 1 predicted that soil depths at Healy and Toolik with the highest previous freeze-thaw frequency (Healy mineral depths and Toolik organic depth) would be composed of more lignin-like and aromatic compounds due to preferential turnover of simple aliphatic compounds during prior freeze-thaw or extended periods of thaw. We infer from the SOM compositions of the organic horizons at the landscape surface that carbon composition and carbon oxidation states may not vary considerably between sites even in cases where annual freeze-thaw differs by 25 freeze-thaw cycles, contradicting Hypothesis 1. Our findings further question the effect of cumulative freeze-thaw cycles on SOM composition, aligning with prior literature that reported negligible differences between concentrations of ammonium (Patel et al., 2021) and microbial biomass carbon (Song et al., 2017) following the first freeze-thaw cycle and subsequent freeze-thaw cycles following a prolonged state of thaw or freezing. The disruption to microbes associated with initial freeze-thaw was well illustrated by the decreasing microbial N and increasing available N reported in high alpine soils in the Lys Vallée of Northwest Italy (Freppaz et al., 2007). These findings have led to the conclusion that most lysis and impact to microbial biomass occurs during the first freeze-thaw cycle, although some potential for additional disturbance and impacts to SOM content and nutrient cycling were reported in the same studies (Freppaz et al., 2007; Song et al., 2017). Our findings contribute a longer timeframe than typically studied. We found that contrasting freeze-thaw cycle frequencies did not result in differences in carbon compound class and oxidation states within FT-ICR-MS resolved SOM compositions.

In contrast to surface soils with large differences in freeze-thaw history, we detected differences in the FT-ICR-MS profile of deeper mineral subsoils with similar freeze-thaw history. This suggests that other factors, such as particle size distribution, may exert stronger control on SOM composition in soils with smaller amounts of prior freeze-thaw. Differences in particle size class can result in contrasting oxygen limitations that may be responsible for differing mineralization rates and selectivity in carbon compound protection (Keiluweit et al., 2017). Specifically, the presence of anaerobic microsites attributed to finer textured soils has been associated with decreased mineralization. However, the higher NOSC of the finer-textured Healy control soils could contradict the selective protection and decreased mineralization described by Keiluweit et al. (2017) in finer particle sizes (25–45 μm) compared with coarser particle sizes (150–250 μm). The response of Healy lower mineral soils to freeze-thaw also showed increased mineralization compared with Toolik soils. Healy's had a larger loss of unique peaks across all compound classes (and complementary increase in respiration shown in Figure S8 of Supporting Information S1) and increase in oxidation in the finer textured soils (Healy samples). Consequently, the differences in SOM composition between Healy and Toolik soils are likely the result of a combination of biogeochemical factors which may have played a role in driving differences in SOM response to experimental freeze-thaw.

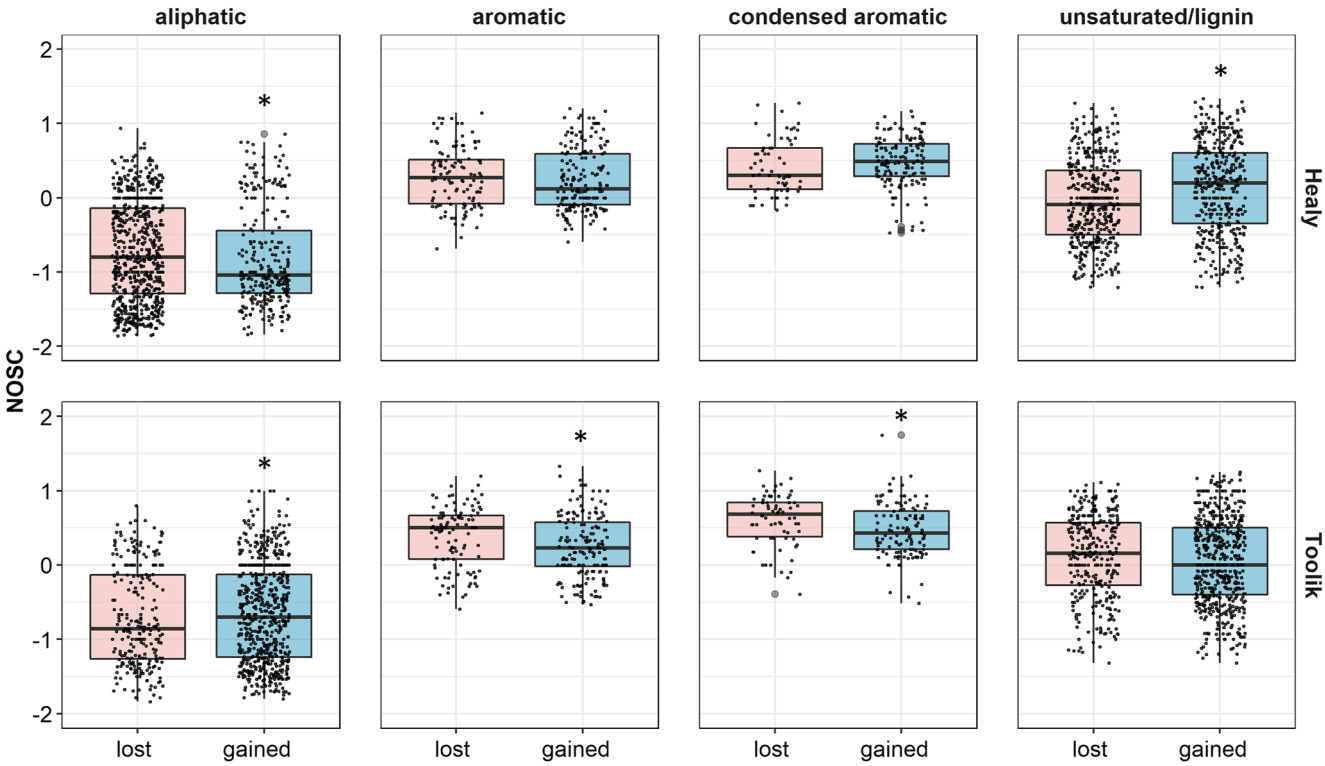

Figure 8. Nominal oxidation state of carbon (NOSC) for compounds lost or gained (newly identified) following freeze-thaw, by site and compound class (all depths). Statistical significance was determined at $\alpha = 0.05$. There were significant increases in the NOSC of gained compounds (compared to lost compounds) in lignin-like compounds in Healy soils and aliphatic compounds in Toolik. There were significant decreases in the NOSC of gained compounds (compared to lost compounds) in Healy aliphatics as well as Toolik aromatics and condensed aromatics.

4.2. SOM Response to Experimental Freeze-Thaw

One of the largest differences in freeze-thaw response occurred between Healy and Toolik samples in the soil depths with the most similar prior freeze-thaw history: lower mineral soil depths (Figure 2; Figures 5–8). The lower mineral soils at Toolik were the only samples to not undergo an overall increase in NOSC following experimental freeze-thaw, although there was an increase in the NOSC of aliphatic molecules (Figures 7 and 8). The lower mineral soils from Healy were the only samples to undergo changes in relative abundance of carbon classes (with lignin-like compounds increasing and aliphatics decreasing) as well as the only samples to lose more carbon compounds than were gained. Total carbon content was similar across lower mineral samples from both sites, which reduces concerns that the FT-ICR-MS analysis protocol did not control the amount of organic matter in each sample injected for analysis. However, we do acknowledge that this protocol does limit the interpretation of changes in peak count.

Hypothesis 2 predicted a loss of aliphatics in soils with little prior freeze-thaw as temperature-driven protection from turnover was lost during experimental freeze-thaw. While we did not observe the expected loss in simple aliphatic molecules, the increase in the NOSC (the oxidation of carbon molecules) of aliphatics in Toolik samples following freeze-thaw, accompanied by a decrease in NOSC in aromatics and condensed aromatics, could indicate that the carbon metabolism in the Toolik lower mineral depth was slower than in Healy soils and distributed across multiple carbon classes rather than targeted at aliphatics. The aliphatic components from Toolik samples showing increased NOSC traits may be intermediate metabolites, not completely oxidized to CO_2. The divergent responses to freeze-thaw by aliphatic and aromatic/condensed aromatic molecules in the Toolik soils could indicate targeted oxidation of both compound groups (compared to selective decomposition of aliphatics only). We posit that, in both sites, microbes consuming the most oxidized aromatic and condensed aromatic molecules may leave behind the less thermodynamically favorable molecules, thus lowering the overall NOSC of aromatic and condensed aromatic pools but still indicating mineralization processes. Meanwhile, microbial oxidation of the

aliphatic pool would increase its thermodynamic favorability for future microbial use as we observed in Toolik soils.

The changes in NOSC at both sites following experimental freeze-thaw indicate that the potential for carbon decomposition in mineral depths increased following repeated freeze-thaw. The results of the supplementary respiration experiment included in our study align with the expected increase in carbon decomposition following freeze-thaw in Healy's lower mineral soils, with freeze-thaw samples from that depth showing the highest production of CO_2 compared with Healy's upper mineral and organic depths. Interestingly, the largest losses of carbon as CO_2 from Toolik soils occurred in the control samples from the lower mineral depths (Figure S8 in Supporting Information S1), with comparable but smaller CO_2 concentrations in the freeze-thaw samples from Toolik. The greater response by Toolik in the supplemental respiration experiment coincides with the slower response of aliphatics to experimental freeze-thaw in Toolik's lower mineral samples (increased NOSC but no difference in relative abundance). Notably, Healy aliphatics decreased in NOSC following experimental freeze-thaw. Similar to aromatic and condensed aromatic molecules from the Toolik soil samples, the decrease in NOSC at Healy may be due to the overall loss of higher NOSC aliphatics following microbial use and respiration. The loss of aliphatics from Healy serves as a potential explanation for the lesser CO_2 production from Healy's lower mineral samples (compared with Toolik samples) during the supplemental respiration experiment (Figure S8 in Supporting Information S1).

The variable responses of aliphatic compounds in the lower mineral horizons from Healy and Toolik following freeze-thaw illuminate differences in soil response to experimental freeze-thaw cycles. Variation in the short-term response of SOM could be introduced by freeze-thaw processes that promote microbial lysis and substrate input as well as disruption to soil aggregation (Freppaz et al., 2007; Oztas & Fayetorbay, 2003). Differences may also be attributed to contrasting site latitudes. Selective utilization of aliphatic compounds (56% loss of aliphatic molecules) for dissolved organic carbon in the active layer from Alaskan soils in discontinuous permafrost was observed during a 28-day bioincubation at 20°C by Textor et al. (2019). The selective utilization of aliphatic compounds observed in a discontinuous permafrost soil may not be occurring in a permafrost soil which has undergone little prior freeze-thaw and is located in higher latitudes with continuous permafrost, such as Toolik. A Siberian permafrost study presenting detailed molecular composition of SOM identified increased bioavailability following thaw of *both* complex and simple carbon compounds in permafrost soils from continuous permafrost zones (Dao et al., 2022). Diverging soil responses under warming compared with freeze-thaw conditions requires further investigation.

4.3. The Role of Mineralogy and Moisture Conditions in Freeze-Thaw Response of SOM in Lower Mineral Soils

Additional factors could be responsible for contrasts in microbial oxidation of carbon and the relative abundance of lignin-like compounds including the higher water content present in the Healy samples as well as differences in iron crystallinity between both sites. In the relatively high-moisture lower mineral soils from Healy, O_2 availability may have been limiting for lignin depolymerization, aligning well with the increased relative abundance of lignin under experimental freeze-thaw. Anaerobic decomposition pathways are often guided by the availability of reactive iron species, allowing for microbial oxidation of carbon in saturated conditions and potentially leading to the diverging FT-ICR-MS profiles in subsoils from both sites with similar freeze-thaw histories but differences in moisture, iron reactivity, and mineralogical composition (Lentini et al., 2012).

The differences in clay content and mineralogy—specifically crystalline versus poorly crystalline iron and aluminum—between sites may have influenced the biogeochemical response to freeze-thaw through contrasting mineral-organic matter interactions. A study by Gentsch et al. (2015) reported slow microbial transformation of organic molecules in permafrost on the scale of millennia. The study attributed the accumulation of SOM in permafrost soils to a combination of microbial transformation and mineral-associations, with reactive iron and aluminum as well as clay minerals adsorbing organic molecules and decreasing availability even under warming conditions (Gentsch et al., 2015). We infer a higher sorption potential in Healy soils based on higher clay content, larger concentrations of poorly crystalline iron and aluminum, and greater concentrations of feldspars such as microcline and albite, as well as mica. Interestingly, the greater loss of aliphatics and overall loss of peaks from lower mineral depths at Healy suggest that some (but not all, i.e., Healy upper mineral and organic) soils containing minerals with more sorption potential showed greater loss of FT-ICR-MS resolved peaks during the experimental

freeze-thaw incubation compared to soils from Toolik containing silicate minerals with lower charge density (quartz) and lower clay contents. These results contrast previous literature which found greater SOM protection through organo-mineral interactions in soils with similar mineralogy and texture as in the Healy soils (Baldock & Skjemstad, 2000; Kögel-Knabner et al., 2008; Sollins et al., 1996), allowing for the possibility that freeze-thaw may be responsible for changing carbon dynamics in newly thawed permafrost with less prior freeze-thaw history. Notably, the Healy soil's upper mineral and organic horizons, which had more prior freeze-thaw than in the lower mineral horizon, did not undergo the same loss of peaks and decrease in aliphatics observed in Healy's lower mineral horizon. The only horizon from the Healy soils to display carbon loss, oxidation, and decrease in aliphatics following freeze-thaw was the lower mineral horizon which had the least prior freeze-thaw.

The interaction of organic carbon and reactive iron is especially relevant in current permafrost research, with a recent study finding that iron-associated organic carbon was ~7% higher in cryoturbated soils compared with non-cryoturbated organic and mineral soils (Joss et al., 2022). While both Healy and Toolik presented evidence for cryoturbation (i.e., Table 1), Healy soils—with a higher proportion of poorly crystalline iron and aluminum—underwent greater loss of FT-ICR-MS resolved carbon peaks compared with Toolik soils. The loss of peaks observed in Healy soils contrasts the expected stabilization of carbon in soils containing both cryoturbation and oxidized poorly crystalline iron species, suggesting that iron-mediated anaerobic decomposition pathways may be a more important control on organic matter stabilization in this system.

However, the direct role of mineral-associated SOM transformation in mediating loss of carbon and decrease in aliphatics from Healy may not be captured by the FT-ICR-MS approach. With 10% SOC in Healy soils, we do not expect the full SOM pool to be extracted and identifiable via FT-ICR-MS (Kim et al., 2022). Our analyses using water-extractable organic matter are likely targeting readily available SOM, which is more vulnerable to microbial action and not as protected by mineral stabilization (Gentsch et al., 2015). While FT-ICR-MS is a powerful technique that offers a glimpse into SOM composition, additional techniques (i.e., density separations, radiocarbon dating) are needed to provide further insight into the role and mechanisms of mineral-associated SOM in freeze-thaw response.

There is potential for impacts to sorption capacity in soil following freeze-thaw. A previous study using geosynthetic clay liners identified mineral dissolution during freeze-thaw as a driver of displacement on cation exchange sites, although these impacts were only seen after 15 to 20 freeze-thaw cycles (Makusa et al., 2014). The study investigated freeze-thaw as a wetting-drying process with the ability to drive changes in hydraulic conductivity and dissolution. Dissolution and ion displacement triggered by freeze-thaw may have altered mineral-organic matter interactions in Healy soils by increasing competition for sorption sites on clay minerals and poorly crystalline iron oxides. Increased dissolution following freeze-thaw and subsequent competition for mineral sorption could partially explain the increasing vulnerability of carbon compounds in Healy samples to microbial mineralization despite previous studies that have found an increase in carbon sorption on clay and mica minerals following freeze-thaw (G.-P. Wang et al., 2007; Yu et al., 2010).

The greater loss of carbon compounds from Healy also aligns with findings from a recent experiment investigating iron mineral and organic carbon interactions during permafrost thaw in Sweden (Patzner et al., 2020). Saturated conditions during permafrost thaw resulted in mobilization of iron and carbon as a result of iron reduction during anaerobic metabolism. In our experiment, the higher ice content (higher water content during the thaw; Table 2) at Healy may have driven waterlogging and anaerobic conditions during experimental freeze-thaw or during prior *in situ* freeze-thaw resulting in reactive iron mineral dissolution and subsequent carbon release, consistent with Patzner et al. (2020). It is also possible that the higher proportion of poorly crystalline iron in Healy soils was more readily reduced in saturated conditions compared with the higher proportion of crystalline iron at Toolik, resulting in microbial oxidation of carbon compounds using poorly crystalline iron as a terminal electron acceptor (Lentini et al., 2012; Lovley & Phillips, 1988). Previous studies using laboratory incubations of non-permafrost soil from the Northeastern United States (Lovley & Phillips, 1988) have identified the association of poorly crystalline iron (ferrihydrite) with increased rates of Fe (III) reduction compared with highly crystalline iron (goethite). These potential explanations for the rapid loss of the aliphatic pool following experimental freeze-thaw highlight the importance of reactive iron oxide minerals in carbon destabilization following permafrost thaw.

Permafrost formation mechanisms also likely contributed to the higher thermodynamic favorability of the lower mineral horizons at Healy in addition to the influence of differences in mineralogical abundance between sites. Older permafrost is reported to be more decomposable than younger permafrost on the basis of ammonium concentration, microbial scavenging, as well as fermentation genes and bioproducts increasing with permafrost age (Leewis et al., 2020). However, we posit that permafrost with freeze-thaw history in the form of quasi-syngenetic permafrost; i.e., the upward growth of permafrost into already accumulated peats and sediment (Kanevskiy, 2003; Manies et al., 2021), may result in highly oxygenated carbon compounds primed for rapid decomposition and loss once thaw occurs as seen in the lower mineral depths from Healy. Our interpretation corresponds to prior work conducted in the discontinuous permafrost zone in Fairbanks, Alaska that compared carbon losses from two sites with contrasting permafrost formation (syngenetic vs. quasi-syngenetic) (Manies et al., 2021). The degree of peat decomposition prior to permafrost formation heavily influenced the biolability of organic compounds following permafrost thaw (Manies et al., 2021). Specifically, the manner of permafrost formation (if permafrost formed with or following peat deposition), influenced C:N ratio, with soils that underwent peat formation and microbial decomposition prior to permafrost formation (epigenetic and quasi-syngenetic permafrost) having lower C:N ratios compared with soil that underwent peat and permafrost formation simultaneously (syngenetic permafrost) (Manies et al., 2021). Since the soil morphology at both Toolik and Healy indicates cryoturbation in the lower mineral permafrost horizons, it is possible that both sites underwent either quasi-syngenetic or epigenetic permafrost formation. However, the SOC composition of the control soils indicates higher thermodynamic favorability in Healy, suggesting that processes preceding permafrost formation at the Healy site may have resulted in higher NOSC values and more vulnerable aliphatics compared to Toolik soils. These processes could reflect timing (how long peat decomposed prior to permafrost aggradation) or the contrasting soil characteristics including mineralogy and iron and aluminum crystallinity.

5. Conclusions

Our findings indicate that a combination of freeze-thaw history and soil properties may dictate soil response to future freeze-thaw cycles. Lower mineral soils from Healy and Toolik with the least prior freeze-thaw history had diverging FT-ICR-MS resolved soil chemistry responses to future freeze-thaw cycles, likely as a function of differences in soil moisture and mineralogy. Specifically, lower mineral soils from Healy (a lower latitude permafrost soil with higher freeze-thaw cycle frequency at upper depths) appeared to have more short-term carbon metabolism within the aliphatic pool compared to soils from Toolik (a higher latitude permafrost soil with lower freeze-thaw cycle frequency at upper depths) following experimental freeze-thaw, resulting in a net loss of carbon compounds in Healy soils. Based on these findings, we posit that future increases in freeze-thaw in both the active layer and thawing permafrost may result in contrasting carbon response depending on site-specific characteristics, such as oxygen-availability following thaw, concentrations of reactive iron and aluminum, and prior permafrost formation processes. Interactions among texture, mineralogy, saturation, Fe and Al reactivity, and nutrient regimes likely vary based on freeze-thaw history as demonstrated by the contrasting SOM response between the upper and lower mineral horizons of Healy soils. Understanding freeze-thaw in warming Arctic landscapes is central to predicting how thawing permafrost will behave in the coming decades, with implications for carbon respiration and greenhouse gas release. The variation in freeze-thaw response across the Arctic has the potential to further complicate our predictive abilities, necessitating further study of how previous site-specific freeze-thaw may alter biogeochemical processes during thaw.

Data Availability Statement

All data and scripts are available at https://github.com/Erin-Rooney/FTC-FTICR and are archived and searchable at https://search.emsl.pnnl.gov (Project ID #50267).

Acknowledgments
The authors would like to thank David Myrold, Jeff Hatten, Jennifer Fedenko, Ruben Aleman, Holly Golightly, Mark Bowden, Tom Wietsma, Rosalie K. Chu, Jason Toyoda, and Ashley Waggoner for their expertise and assistance with this experiment. The authors would like to thank Adam Fund, Kristin McAdow, and the Soil Health Laboratory at Oregon State University for their help with soil characterization analyses. The authors would also like to thank the anonymous peer reviewer for their contributions and valuable insight. This research was supported by the U.S. Department of Energy, Office of Science, Biological and Environmental Research as part of the Environmental System Science Program. The Pacific Northwest National Laboratory is operated for DOE by Battelle Memorial Institute under contract DE-AC05-76RL01830. A portion of this research was performed using EMSL (grid.436923.9), a DOE Office of Science user facility sponsored by the Department of Energy's Office of Biological and Environmental Research and located at Pacific Northwest National Laboratory. This material is based in part upon work supported by NSF through the NEON program. NEON is sponsored by the National Science Foundation (NSF) and operated under cooperative agreement by Battelle.

References

Antony, R., Willoughby, A. S., Grannas, A. M., Catanzano, V., Sleighter, R. L., Thamban, M., et al. (2017). Molecular Insights on Dissolved Organic Matter Transformation by Supraglacial Microbial Communities. *Environmental Science & Technology*, *51*(8), 4328–4337. https://doi.org/10.1021/acs.est.6b05780

Arndt, K. A., Lipson, D. A., Hashemi, J., Oechel, W. C., & Zona, D. (2020). Snow melt stimulates ecosystem respiration in Arctic ecosystems. *Global Change Biology*, *26*(9), 5042–5051. https://doi.org/10.1111/gcb.15193

Bailey, V. L., Pries, C. H., & Lajtha, K. (2019). What do we know about soil carbon destabilization? *Environmental Research Letters*, *14*(8), 083004. https://doi.org/10.1088/1748-9326/ab2c11

Baldock, J. A., & Skjemstad, J. O. (2000). Role of the soil matrix and minerals in protecting natural organic materials against biological attack. *Organic Geochemistry*, *31*, 697–710. https://doi.org/10.1016/s0146-6380(00)00049-8

Bing, H., He, P., & Zhang, Y. (2015). Cyclic freeze–thaw as a mechanism for water and salt migration in soil. *Environmental Earth Sciences*, *74*(1), 675–681. https://doi.org/10.1007/s12665-015-4072-9

Blackwell, M. S. A., Brookes, P. C., delaFuente-Martinez, N., Gordon, H., Murray, P. J., Snars, K. E., et al. (2010). Phosphorus Solubilization and Potential Transfer to Surface Waters from the Soil Microbial Biomass Following Drying–Rewetting and Freezing–Thawing. *Advances in Agronomy*. Academic Press Inc. https://doi.org/10.1016/S0065-2113(10)06001-3

Boswell, E. P., Balster, N. J., Bajcz, A. W., & Thompson, A. M. (2020a). Soil aggregation returns to a set point despite seasonal response to snow manipulation. *Geoderma*, *357*, 113954. https://doi.org/10.1016/j.geoderma.2019.113954

Boswell, E. P., Thompson, A. M., Balster, N. J., & Bajcz, A. W. (2020b). Novel determination of effective freeze–thaw cycles as drivers of ecosystem change. *Journal of Environmental Quality*, *49*(2), 314–323. https://doi.org/10.1002/jeq2.20053

Brosgé, W. P., Reiser, H. N., Dutro, J. T., Jr., Detterman, R. L., & Tailleur, I. L. (2001). *Geologic map of the Arctic Quadrangle, Alaska: U.S. Geological Survey Geologic Investigations Series Map 2673* (p. 381). U.S. Geological Survey.

Butler, B., Hillier, S., Beaudette, D., & Eberl, D. (2021). *Full Pattern Summation of X-Ray Powder Diffraction Data*. PowdR. CRAN Repository.

Chou, Y., & Wang, L. (2021). Seasonal freezing-thawing process and hydrothermal characteristics of soil on the Loess Plateau, China. *Journal of Mountain Science*, *18*(11), 3082–3098. https://doi.org/10.1007/s11629-020-6599-9

Csejtey, B., Jr., Mullen, M. W., Cox, D. P., & Stricker, G. D. (1992). *Geology and geochronology of the Healy Quadrangle, south-central Alaska*. https://doi.org/10.3133/i1961

Dao, T. T., Mikutta, R., Sauheitl, L., Gentsch, N., Shibistova, O., Wild, B., et al. (2022). Lignin Preservation and Microbial Carbohydrate Metabolism in Permafrost Soils. *Journal of Geophysical Research: Biogeosciences*, *127*(1). https://doi.org/10.1029/2020JG006181

Dittmar, T., Koch, B., Hertkorn, N., & Kattner, G. (2008). A simple and efficient method for the solid-phase extraction of dissolved organic matter (SPE-DOM) from seawater. *Limnology and Oceanography: Methods*, *6*(6), 230–235. https://doi.org/10.4319/lom.2008.6.230

Edwards, L. M. (2013). The effects of soil freeze–thaw on soil aggregate breakdown and concomitant sediment flow in Prince Edward Island: A review. *Canadian Journal of Soil Science*, *93*(4), 459–472. https://doi.org/10.4141/cjss2012-059

Elliott, A. C., & Henry, H. A. L. (2009). Freeze-thaw cycle amplitude and freezing rate effects on extractable nitrogen in a temperate old field soil. *Biology and Fertility of Soils*, *45*(5), 469–476. https://doi.org/10.1007/s00374-009-0356-0

Freppaz, M., Williams, B. L., Edwards, A. C., Scalenghe, R., & Zanini, E. (2007). Simulating soil freeze/thaw cycles typical of winter alpine conditions: Implications for N and P availability. *Applied Soil Ecology*, *35*(1), 247–255. https://doi.org/10.1016/j.apsoil.2006.03.012

Gao, Z., Hu, X., Li, X.-Y., & Li, Z.-C. (2021). Effects of freeze-thaw cycles on soil macropores and its implications on formation of hummocks in alpine meadows in the Qinghai Lake watershed, northeastern Qinghai-Tibet Plateau. *Journal of Soils and Sediments*, *21*(1). https://doi.org/10.1007/s11368-020-02765-2

Gee, G. W., & Bauder, J. W. (1986). Particle-size analysis. In A. Klute (Ed.), *Methods of soil analysis. Part 1*, *Agron. Monogr. 9* (2nd ed., pp. 383–411). ASA and SSSA.

Gentsch, N., Mikutta, R., Shibistova, O., Wild, B., Schnecker, J., Richter, A., et al. (2015). Properties and bioavailability of particulate and mineral-associated organic matter in Arctic permafrost soils, Lower Kolyma Region, Russia. *European Journal of Soil Science*, *66*(4), 722–734. https://doi.org/10.1111/ejss.12269

Graham, E. B., Tfaily, M. M., Crump, A. R., Goldman, A. E., Bramer, L. M., Arntzen, E., et al. (2017). Carbon inputs from riparian vegetation limit oxidation of physically bound organic carbon via biochemical and thermodynamic processes. *Journal of Geophysical Research: Biogeosciences*, *122*(12), 3188–3205. https://doi.org/10.1002/2017JG003967

Guo, D., & Wang, H. (2013). Simulation of permafrost and seasonally frozen ground conditions on the Tibetan Plateau, 1981-2010. *Journal of Geophysical Research: Atmospheres*, *118*(11), 5216–5230. https://doi.org/10.1002/jgrd.50457

Henry, H. A. L. (2007). Soil freeze-thaw cycle experiments: Trends, methodological weaknesses and suggested improvements. *Soil Biology and Biochemistry*, *39*, 977–986. https://doi.org/10.1016/j.soilbio.2006.11.017

Henry, H. A. L. (2008). Climate change and soil freezing dynamics: Historical trends and projected changes. *Climatic Change*, *87*(3–4), 421–434. https://doi.org/10.1007/s10584-007-9322-8

Joss, H., Patzner, M. S., Maisch, M., Mueller, C. W., Kappler, A., & Bryce, C. (2022). Cryoturbation impacts iron-organic carbon associations along a permafrost soil chronosequence in northern Alaska. *Geoderma*, *413*, 115738. https://doi.org/10.1016/j.geoderma.2022.115738

Kanevskiy, M. (2003). *Cryogenic structure of mountain slope deposits, northeast Russia*. *Paper Presented at the 8th International Conference on Permafrost*.

Keiluweit, M., Wanzek, T., Kleber, M., Nico, P., & Fendorf, S. (2017). Anaerobic microsites have an unaccounted role in soil carbon stabilization. *Nature Communications*, *8*(1), 1771. https://doi.org/10.1038/s41467-017-01406-6

Kim, S., Kim, D., Jung, M., & Kim, S. (2022). Analysis of environmental organic matters by ultrahigh-resolution mass spectrometry—A review on the development of analytical methods. *Mass Spectrometry Reviews*, *41*(2), 352–369. https://doi.org/10.1002/mas.21684

Koch, B. P., & Dittmar, T. (2006). From mass to structure: An aromaticity index for high-resolution mass data of natural organic matter. *Rapid Communications in Mass Spectrometry*, *20*(5), 926–932. https://doi.org/10.1002/rcm.2386

Kögel-Knabner, I., Guggenberger, G., Kleber, M., Kandeler, E., Kalbitz, K., Scheu, S., et al. (2008). Organo-mineral associations in temperate soils: Integrating biology, mineralogy, and organic matter chemistry. *Journal of Plant Nutrition and Soil Science*, *171*(1), 61–82. https://doi.org/10.1002/jpln.200700048

Köhn, M. (1928). Bemerkungen zur mechanischen Bodenanalyse. III. Ein neuer Pipettapparat. *Zeitschrift Für Pflanzenernährung, Düngung, Bodenkunde, A, Wissenschaftlicher Teil*, *11*(1), 50–54. https://doi.org/10.1002/jpln.19280110104

Konrad, J.-M., & McCammon, A. W. (1990). Solute partitioning in freezing soils. *Canadian Geotechnical Journal*, *27*(6), 726–736. https://doi.org/10.1139/t90-086

Kujawinski, E. B., & Behn, M. D. (2006). Automated analysis of electrospray ionization fourier transform ion cyclotron resonance mass spectra of natural organic matter. *Analytical Chemistry*, *78*(13), 4363–4373. https://doi.org/10.1021/ac0600306

Kujawinski, E. B., Hatcher, P. G., & Freitas, M. A. (2002). High-resolution fourier transform ion cyclotron resonance mass spectrometry of humic and fulvic acids: Improvements and comparisons. *Analytical Chemistry*, *74*(2), 413–419. https://doi.org/10.1021/ac0108313

LaRowe, D. E., & van Cappellen, P. (2011). Degradation of natural organic matter: A thermodynamic analysis. *Geochimica et Cosmochimica Acta*, *75*(8), 2030–2042. https://doi.org/10.1016/j.gca.2011.01.020

Larsen, K. S., Jonasson, S., & Michelsen, A. (2002). Repeated freeze-thaw cycles and their effects on biological processes in two arctic ecosystem types. *Applied Soil Ecology*, *21*. https://doi.org/10.1016/s0929-1393(02)00093-8

Lawlor, J. (2020). *PNWColors: Color Palettes Inspired by Nature in the US Pacific Northwest*. Zenodo.
Leewis, M.-C., Berlemont, R., Podgorski, D. C., Srinivas, A., Zito, P., Spencer, R. G. M., et al. (2020). Life at the Frozen Limit: Microbial Carbon Metabolism Across a Late Pleistocene Permafrost Chronosequence. *Frontiers in Microbiology*, *11*. https://doi.org/10.3389/fmicb.2020.01753
Lentini, C. J., Wankel, S. D., & Hansel, C. M. (2012). Enriched Iron(III)-Reducing Bacterial Communities are Shaped by Carbon Substrate and Iron Oxide Mineralogy. *Frontiers in Microbiology*, *3*. https://doi.org/10.3389/fmicb.2012.00404
Liu, B., Ma, R., & Fan, H. (2021). Evaluation of the impact of freeze-thaw cycles on pore structure characteristics of black soil using X-ray computed tomography. *Soil and Tillage Research*, *206*, 104810. https://doi.org/10.1016/j.still.2020.104810
Lovley, D. R., & Phillips, E. J. P. (1988). Novel mode of microbial energy metabolism: Organic carbon oxidation coupled to dissimilatory reduction of iron or manganese. *Applied and Environmental Microbiology*, *54*(6), 1472–1480. https://doi.org/10.1128/aem.54.6.1472-1480.1988
Ma, R., Jiang, Y., Liu, B., & Fan, H. (2021). Effects of pore structure characterized by synchrotron-based micro-computed tomography on aggregate stability of black soil under freeze-thaw cycles. *Soil and Tillage Research*, *207*, 104855. https://doi.org/10.1016/j.still.2020.104855
MacDonald, E. N., Tank, S. E., Kokelj, S. v., Froese, D. G., & Hutchins, R. H. S. (2021). Permafrost-derived dissolved organic matter composition varies across permafrost end-members in the western Canadian Arctic. *Environmental Research Letters*, *16*(2), 024036. https://doi.org/10.1088/1748-9326/abd971
Makusa, G. P., Bradshaw, S. L., Berns, E., Benson, C. H., & Knutsson, S. (2014). Freeze–thaw cycling concurrent with cation exchange and the hydraulic conductivity of geosynthetic clay liners. *Canadian Geotechnical Journal*, *51*(6), 591–598. https://doi.org/10.1139/cgj-2013-0127
Manies, K. L., Jones, M. C., Waldrop, M. P., Leewis, M., Fuller, C., Cornman, R. S., & Hoefke, K. (2021). Influence of permafrost type and site history on losses of permafrost carbon after thaw. *Journal of Geophysical Research: Biogeosciences*, *126*(11). https://doi.org/10.1029/2021JG006396
Miller, R. O., Gavlak, R., & Horneck, D. (2013). *Soil, Plant, and Water Reference Methods for the Western Region* (4th ed.).
National Ecological Observatory Network. (2019). *Terrestrial Observation System (TOS) Site Characterization Report: Domain 18*. https://doi.org/10.10179/2263491
National Ecological Observatory Network. (2020). *Soil physical and chemical properties, distributed initial characterization*. Accessed on 6 October 2020.
National Ecological Observatory Network. (2021). *Soil temperature (DP1.00041.001)*. Accessed 27 July 2021.
Oksanen, J., Blanchet, F. G., Friendly, M., Kindt, R., Legendre, P., McGlinn, D., et al. (2019). *Vegan: Community Ecology Package. R Package*.
Oztas, T., & Fayetorbay, F. (2003). Effect of freezing and thawing processes on soil aggregate stability. *CATENA*, *52*(1), 1–8. https://doi.org/10.1016/S0341-8162(02)00177-7
Park, H., Fedorov, A. N., Zheleznyak, M. N., Konstantinov, P. Y., & Walsh, J. E. (2015). Effect of snow cover on pan-Arctic permafrost thermal regimes. *Climate Dynamics*, *44*(9–10), 2873–2895. https://doi.org/10.1007/s00382-014-2356-5
Patel, K. F. (2020). *fticrrr. R Package*. Zenodo. https://doi.org/10.5281/zenodo.3893246
Patel, K. F., Tatariw, C., MacRae, J. D., Ohno, T., Nelson, S. J., & Fernandez, I. J. (2018). Soil carbon and nitrogen responses to snow removal and concrete frost in a northern coniferous forest. *Canadian Journal of Soil Science*, *98*(3), 436–447. https://doi.org/10.1139/cjss-2017-0132
Patel, K. F., Tatariw, C., MacRae, J. D., Ohno, T., Nelson, S. J., & Fernandez, I. J. (2021). Repeated freeze–thaw cycles increase extractable, but not total, carbon and nitrogen in a Maine coniferous soil. *Geoderma*, *402*, 115353. https://doi.org/10.1016/j.geoderma.2021.115353
Patzner, M. S., Mueller, C. W., Malusova, M., Baur, M., Nikeleit, V., Scholten, T., et al. (2020). Iron mineral dissolution releases iron and associated organic carbon during permafrost thaw. *Nature Communications*, *11*(1), 6329. https://doi.org/10.1038/s41467-020-20102-6
Ping, C. L., Jastrow, J. D., Jorgenson, M. T., Michaelson, G. J., & Shur, Y. L. (2015). Permafrost soils and carbon cycling. *SOIL*, *1*(1), 147–171. https://doi.org/10.5194/soil-1-147-2015
R Core Team. (2020). *R: A language and environment for statistical computing*.
Rooney, E. C., Bailey, V. L., Patel, K. F., Dragila, M., Battu, A. K., Buchko, A. C., et al. (2022). Soil pore network response to freeze-thaw cycles in permafrost aggregates. *Geoderma*, *411*, 115674. https://doi.org/10.1016/j.geoderma.2021.115674
Schimel, J. P., & Clein, J. S. (1996). Microbial response to freeze-thaw cycles IN tundra and TAIGA soils. *Soil Eiot. Biorhem*, *28*. https://doi.org/10.1016/0038-0717(96)00083-1
Schimel, J. P., & Mikan, C. (2005). Changing microbial substrate use in Arctic tundra soils through a freeze-thaw cycle. *Soil Biology and Biochemistry*, *37*(8), 1411–1418. https://doi.org/10.1016/j.soilbio.2004.12.011
Seidel, M., Beck, M., Riedel, T., Waska, H., Suryaputra, I. G. N. A., Schnetger, B., et al. (2014). Biogeochemistry of dissolved organic matter in an anoxic intertidal creek bank. *Geochimica et Cosmochimica Acta*, *140*, 418–434. https://doi.org/10.1016/j.gca.2014.05.038
Shang, C., & Zelazny, L. W. (2015). *Selective dissolution techniques for mineral analysis of soils and sediments* (pp. 33–80). https://doi.org/10.2136/sssabookser5.5.c3
Sharratt, B. S., Baker, D. G., Wall, D. B., Skaggs, R. H., & Ruschy, D. L. (1992). Snow depth required for near steady-state soil temperatures. *Agricultural and Forest Meteorology*, *57*(4), 243–251. https://doi.org/10.1016/0168-1923(92)90121-J
Sheldrick, B. H., & Wang, C. (1993). Particle Size Analysis. In M. R. Carter (Ed.), *Soil Sampling and Methods of Analysis* (pp. 499–517). Lewis Publishers.
Soil Science Division Staff. (2017). Soil survey manual. In C. Ditzler, K. Scheffe, & H. C. Monger (Ed.), *USDA Handbook 18*. Government Printing Office.
Soil Survey Staff. (2014). *Keys to Soil Taxonomy, 12th ed*. USDA-Natural Resources Conservation Service.
Sollins, P., Homann, P., & Caldwell, B. A. (1996). Stabilization and destabilization of soil organic matter: Mechanisms and controls. *Geoderma*(74), 65–105. https://doi.org/10.1016/s0016-7061(96)00036-5
Song, Y., Zou, Y., Wang, G., & Yu, X. (2017). Altered soil carbon and nitrogen cycles due to the freeze-thaw effect: A meta-analysis. *Soil Biology and Biochemistry*, *109*, 35–49. https://doi.org/10.1016/j.soilbio.2017.01.020
Textor, S. R., Wickland, K. P., Podgorski, D. C., Johnston, S. E., & Spencer, R. G. M. (2019). Dissolved Organic Carbon Turnover in Permafrost-Influenced Watersheds of Interior Alaska: Molecular Insights and the Priming Effect. *Frontiers of Earth Science*, *7*. https://doi.org/10.3389/feart.2019.00275
Thomas, G. W. (2018). *Soil pH and Soil Acidity* (pp. 475–490). https://doi.org/10.2136/sssabookser5.3.c16
Tolić, N., Liu, Y., Liyu, A., Shen, Y., Tfaily, M. M., Kujawinski, E. B., et al. (2017). Formularity: Software for Automated formula assignment of natural and other organic matter from ultrahigh-resolution mass spectra. *Analytical Chemistry*, *89*(23), 12659–12665. https://doi.org/10.1021/acs.analchem.7b03318
von Lützow, M., Kögel-Knabner, I., Ekschmitt, K., Flessa, H., Guggenberger, G., Matzner, E., & Marschner, B. (2007). SOM fractionation methods: Relevance to functional pools and to stabilization mechanisms. *Soil Biology and Biochemistry*, *39*(9), 2183–2207. https://doi.org/10.1016/j.soilbio.2007.03.007

Wang, G.-P., Liu, J.-S., Zhao, H.-Y., Wang, J.-D., & Yu, J.-B. (2007). Phosphorus sorption by freeze–thaw treated wetland soils derived from a winter-cold zone (Sanjiang Plain, Northeast China). *Geoderma*, *138*(1–2), 153–161. https://doi.org/10.1016/j.geoderma.2006.11.006

Wang, J., Luo, S., Li, Z., Wang, S., & Li, Z. (2019). The freeze/thaw process and the surface energy budget of the seasonally frozen ground in the source region of the Yellow River. *Theoretical and Applied Climatology*, *138*(3–4), 1631–1646. https://doi.org/10.1007/s00704-019-02917-6

Wang, J., Song, C., Hou, A., & Wang, L. (2014). CO2 emissions from soils of different depths of a permafrost peatland, Northeast China: Response to simulated freezing–thawing cycles. *Journal of Plant Nutrition and Soil Science*, *177*(4), 524–531. https://doi.org/10.1002/jpln.201300309

Wickham, H. (2016). *ggplot2: Elegant Graphics for Data Analysis*. Springer.

Wickham, H., François, R., & Henry, L. (2020). *dplyr: A grammar of Data Manipulation*.

Wilson, F. H., Hults, C. P., Mull, C. G., & Karl, S. M. (2015). *Geologic map of Alaska: U.S. Geological Survey Scientific Investigations Map 3340, pamphlet 196* (p. 2). USGS.

Yi, Y., Kimball, J. S., Rawlins, M. A., Moghaddam, M., & Euskirchen, E. S. (2015). The role of snow cover affecting boreal-arctic soil freeze-thaw and carbon dynamics. *Biogeosciences*, *12*(19), 5811–5829. https://doi.org/10.5194/bg-12-5811-2015

Yu, X., Zhang, Y., Zhao, H., Lu, X., & Wang, G. (2010). Freeze-thaw effects on sorption/desorption of dissolved organic carbon in wetland soils. *Chinese Geographical Science*, *20*(3), 209–217. https://doi.org/10.1007/s11769-010-0209-7